Commitment Constraints and the Yang–Mills Mass Gap in VERSF

Abelian phase pinning, retained spectra and conditional continuum bounds

Keith Taylor | VERSF Theoretical Physics Programme

Summary for general readers

A mass gap is a minimum energy needed to excite a system above its lowest-energy state, the vacuum. VERSF proposes that committed facts restrict which changes remain physically possible. This paper tests whether those restrictions, together with the dynamics, prevent excitations of arbitrarily low energy.

The calculations identify both a limitation and a conditional positive result. Keeping every closed-loop record can still allow coordinated motion that becomes arbitrarily cheap in a larger system. A finite restoring force on the relative record phase removes that motion in the specified model; a rigid lock is its limiting case. The gap is an explicit function of the restoring strengths and inertia. With the current treated algebraically, no independent current inertia is needed. The physical mass scale remains an input.

The positive bound survives unlimited volume and finer resolution when the stated physical coefficients remain fixed. Exact coarse graining protects retained responses. The full relaxation spectrum is also protected if every unresolved fibre has a uniform local relaxation gap, or the unresolved distinctions are physically irrelevant and removed. What remains is to derive the coefficients and physical states from VERSF's dynamics and control the interacting vacuum. The paper establishes conditional Abelian Gaussian results, not the pure Yang–Mills mass gap.

Abstract

We study commitment constraints and spectral bounds in a specified field–current–record model. Exact blocking corrects the derivative-only argument: an integrated Laplacian is a boundary term, and the blocked Hessian contains covariance subtraction. Reversible exact grouping splits retained and hidden relaxation spectra. A uniform within-fibre Poincaré bound controls the hidden sector; a continuation-faithful quotient can instead remove invisible distinctions. In the spatial Abelian restriction, closed-loop retention leaves a coordinated soft mode. Finite relative-phase pinning gives a gapped family connecting that parent to a hard-locked Stueckelberg-type mass term. Eliminating an algebraic current gives a closed two-field gap formula and, for equal transverse gradient and inertial coefficients, exactly relativistic transverse dispersion. The longitudinal sector and the complete auxiliary theory remain nonrelativistic. The stated fixed-physical-coefficient Gaussian families have volume- and regulator-stable gaps, time reflection positivity, a unique vacuum and temporal exponential clustering. A scorecard separates these properties from the full Yang–Mills existence requirements. The mass, pinning and field kinetics remain inputs whose physical selection and refinement scaling must be supplied. These are conditional Gaussian results, not a construction of interacting four-dimensional pure Yang–Mills theory.

Table of contents

Summary for general readers 1

Abstract 1

1 The physical question and the status of the results 4

Notation 5

2 Correcting the action and the blocking calculation 6

2.1 Total derivatives and independent operators 6

2.2 The exact blocked action Hessian 6

2.3 Transporting coefficients between scales 7

3 Why local stiffness does not establish a bulk gap 7

3.1 The derivative control 7

3.2 Positive density and rare empty regions 7

3.3 The oscillation estimate and threshold algebra 8

4 What exact coarse graining preserves 8

4.1 Temporal blocking and physical energy 8

4.2 Gaussian and compact group controls 9

4.3 Exact protection of the complete retained response 9

4.4 A preserved retained response with a vanishing fine gap 10

4.5 A uniform fibre gap controls the hidden sector 12

5 Information balance and exact commitment constraints 13

5.1 An exact information identity 13

5.2 The selected primitive carrier and allowed operations 13

5.3 What the native record and renewal results preserve 14

6 Why a live record can preserve a soft mode 15

7 The published spatial field, current and record action 15

7.1 An explicit test of every closed loop 17

7.2 The native neutral reference and physical admission 17

7.3 Different comparison spaces require different tests 18

8 Abelian phase pinning and conditional gaps 18

8.1 Hard locking and the Stueckelberg mass term 18

8.2 Dependence on current inertia 20

8.3 Finite pinning connects the soft and locked models 20

8.4 The algebraic-current theorem 22

8.5 Relation to rigorous Higgs-phase results 23

9 Restoring strength, inertia and the common dynamics 24

9.1 The declared Gaussian transfer 24

9.2 Derive both coefficients from one coupled kernel 24

9.3 The same quantum spectrum supplies both responses 25

9.4 The restoring strength and inertia of the surviving mode 26

9.5 Continuity induces density inertia without a current oscillator 27
9.6 Internal current inertia and the limits of a stiffness ratio 27
9.7 Reconstruct both forms from one history law 28
9.8 What these derivations physically select 28
10 Infinite volume and removal of the regulators 29
10.1 A specified family in physical units 29
10.2 Conditional Gaussian continuum theorem 29
10.3 Executed volume and regulator tests 30
10.4 Axiom scorecard and temporal positivity 31
11 Scaling and interaction conditions that remain essential 33
11.1 Physical normalisation and collapsing positive coefficients 33
11.2 Positive interactions and the changing vacuum 34
11.3 Relation to the strong-sector papers 34
12 Validation and reproducibility 34
13 The remaining physical derivation 37
Conclusion 38
Appendix A Disposition of the superseded claims 38
Appendix B Auxiliary currents, kinetic geometry and measure 39
B.1 Auxiliary-current reconstruction 39
B.2 The complete coordinate metric and reference measure 39
References 40

1 The physical question and the status of the results

The Yang–Mills problem concerns a nontrivial quantum theory in four-dimensional spacetime for a compact simple gauge group, together with a positive energy gap above the vacuum [1]. The excitations in this statement are physical gauge-invariant states. A frequency assigned to a gauge-fixed coordinate is not automatically such an excitation. The pure non-Abelian target must also be separated from a theory that contains photons or independent matter and record fields.

$$H_{\mathrm{phys}} - E_0 \geqslant \Delta(I - P_{\mathrm{vac}}), \qquad \Delta > 0.$$

Here the inequality is a quadratic-form statement on the physical Hilbert space and P_{vac} projects onto its vacuum sector. When uniqueness is part of the target, that sector must be one dimensional. A lattice argument must control the gap in physical energy units as the spatial volume grows and the regulator is removed, while also constructing the limiting theory and vacuum.

Three distinct statements recur below. A positive static Hessian controls a quadratic potential. A normal-mode frequency also depends on the kinetic metric. A quantum Hamiltonian gap requires an admitted Hilbert space, a vacuum and dynamics. We connect these statements explicitly for the Gaussian construction; we do not transfer that connection to an unspecified interacting theory.

Result	**Status**
Exact blocking identities and counterexamples to the old derivative argument	Established for the stated mathematical models
Complete retained response under compatible refinement	Exact under reversibility and the stated grouping identity; does not bound unresolved fine motions
Full relaxation gap under fibre control	Bounded below by the smaller of the retained gap and the minimum within-fibre Poincaré constant
Primitive fact carrier and exact record-preserving operations	Inherited from the cited VERSF results, with their stated premises
Soft modes preserving every spatial closed-loop record	Derived in the published phase restriction; physical admission remains to be established
Native neutral reference and flat transport	The finite flat zero-current family is gauge; identification with the scalar soft witness is not established
Restoring strength and induced inertia from a common response	Derived and checked, including mixed terms; primitive physical kinetics remains an input
Soft-mode bound with general positive mixed inertia	Proved when the surviving direction has a kinetic norm bounded away from zero
Gap under hard locking or finite pinning	Proved for the declared Abelian Gaussian action and kinetic completion; the mass scale is an input

Result	Status
Algebraic current and continuum transverse branches	Closed two-field gap; exactly relativistic transverse dispersion for equal gradient coefficients, with a nonrelativistic longitudinal sector
Infinite-volume Gaussian continuum gap	Constructed for the declared fixed-physical-coefficient family
Physical four-dimensional Yang–Mills mass gap	Not established by these results

The hard-lock unit benchmark has gap $\sqrt{(3-\sqrt{5})/2} \simeq 0.618$ only for the stated unit field and current inertias. It changes to one when the current is algebraic; Section 8.2 gives the continuous dependence. Neither value is a universal VERSF constant. The GeV estimates in the two earlier papers [2,3] are withdrawn as predictions of this mechanism. Appendix A records which earlier claims are superseded.

Notation

Symbol	Meaning
$q = \lvert d \rvert^2$	Spatial Laplacian eigenvalue; $q_\varepsilon(k)$ includes physical spacing
λ_6	Dimension-six coupling in Sections 2–3 and Figure 1
$\mathcal{C}$ and L	Conditional averaging and lift in Section 4
$\mathcal{R}$ and B_{cyc}	Spatial curl symbol and graph cycle matrix
η, ν_0 and $\lvert 0 \rangle$	Completion coordinate, native neutral reference and vacuum state
$\mathcal{W}$ and ω	Frequency operator and scalar frequency
ρ and m_u	Record-phase pinning coefficient and current inertia
K_{zz}, W_2 and G_E	Eliminated stiffness block, source contact operator and Euclidean covariance
m_{f} and $\beta_\pm$	Equal field/record inertia and native onsite stiffness eigenvalues
κ_x and γ_{hid}	Within-fibre Poincaré constant and hidden relaxation gap

2 Correcting the action and the blocking calculation

2.1 Total derivatives and independent operators

Write $s(x) = \mathrm{tr}\big(F_{\mu\nu}F_{\mu\nu}\big)$. The scalar $\partial^2 s$ is gauge invariant and has engineering dimension six in four spacetime dimensions. These facts do not make its constant-coefficient integral an independent bulk interaction.

$$\int_{\mathbb{T}^4} \partial^2 s \, d^4x = 0, \qquad \int_{\mathbb{R}^4} \partial^2 s \, d^4x = 0 \quad \text{with suitable decay.}$$

Proposition 2.1. On a periodic lattice, the sum of the lattice Laplacian of any site scalar is zero. Therefore the corresponding constant action coupling cannot generate a bulk mass. **Proof.** Each shifted site sum equals the unshifted sum, so all terms cancel. The continuum statements follow by integration by parts. A nonconstant coefficient produces derivatives of that coefficient and defines a different interaction. A local composite insertion at nonzero momentum is likewise different from an integrated action coupling.

For a rotationally invariant CP-even pure-gauge effective action, a useful dimension-six off-shell basis, modulo total derivatives and identities, contains the equation-of-motion square and a cubic field-strength invariant. In a fixed generator convention one may write

$$\mathcal{O}_E = \mathrm{tr}[\big(D_\mu F_{\mu\nu}\big)\big(D_\rho F_{\rho\nu}\big)], \qquad \mathcal{O}_3 = f^{abc} F^a_{\mu\nu} F^b_{\nu\rho} F^c_{\rho\mu}.$$

Their signs and normalisations must be stated in an actual matching calculation. The operator $\big(\mathrm{tr}F^2\big)^2$ has dimension eight. A lattice description with only hypercubic symmetry may need further terms before rotational invariance is restored. Replacing $\partial^2 s$ by $\mathcal{O}_E$ changes the action and does not repair the previous derivation by a change of notation.

The coefficient of $\mathcal{O}_E$ is also sensitive to field redefinitions. Varying the leading action under $A_\nu \mapsto A_\nu + \eta D_\mu F_{\mu\nu}$ shifts an equation-of-motion-square term at first order in η. A consistent perturbative redefinition also changes other operators, the measure and observables. Consequently a mass cannot be read from this coefficient alone. This observation does not permit deleting an arbitrary finite higher-derivative interaction nonperturbatively.

The regulated modulation used in the original paper has a second problem near the trivial vacuum. For fixed $\varepsilon_0 > 0$ and a small field amplitude t, both s and $\partial^2 s$ are of order t^2. Hence the additional density in the following expression begins at order t^4, not order t^2:

$$\left(1 + \frac{\lambda_6}{k^2} \frac{\partial^2 s}{s + \varepsilon_0}\right) s - s = O\big(t^4\big), \qquad A = tA_1.$$

It therefore does not supply the asserted algebraic mass term in the Hessian about $A = 0$. The ratio is not sign definite either. A positive and bounded modulation, when needed, must be established from its definition rather than inferred from $\lambda_6 > 0$.

2.2 The exact blocked action Hessian

Let B denote retained variables, ξ eliminated variables, and $dv(\xi)$ a reference measure independent of B. Assume differentiation under the integral is justified. Define the effective action by exact integration:

$$S_{\mathrm{eff}}(B) = -\log \int e^{-S(B,\xi)} dv(\xi), \qquad \partial_i \partial_j S_{\mathrm{eff}} = \langle S_{ij} \rangle_B - \mathrm{Cov}_B\big(S_i, S_j\big).$$

Proposition 2.2. The covariance contribution is negative semidefinite in this identity. **Proof.** Differentiate the logarithm once to obtain $\partial_i S_{\text{eff}} = \langle S_i \rangle_B$. Differentiating that expectation gives its direct derivative minus the covariance with S_j. If the reference measure depends on B, its logarithmic derivatives must be included as well.

A nonnegative variance therefore does not prove a positive contribution to the effective Hessian. Nor does positivity of an unprojected quadratic form force every coefficient of its derivative expansion to be positive. A valid shell calculation needs a specified operator basis, projection, vertices, gauge treatment, normalisation and remainder. A vertex containing one slow and two fast fields is quadratic, not odd, in the fast field. The previous universal positivity inference is not retained.

2.3 Transporting coefficients between scales

Dimensionless shell contributions must be compared at a common scale. If a dimensionful dimension-six coefficient receives a contribution $da_6 = s(q)d\log q/q^2$ and $\lambda_6(k) = k^2 a_6(k)$, then, neglecting anomalous dimensions and mixing,

$$\lambda_6(k) = \left(\frac{k}{k_0}\right)^2 \lambda_6(k_0) + \int_k^{k_0} \left(\frac{k}{q}\right)^2 s(q)\, d\log q.$$

For constant s and zero initial coupling this is $s[1 - (k/k_0)^2]/2$, rather than an unweighted logarithmic growth. As an arithmetic control, $s = 0.057 \times 2.5$ and $k_0/k = 6$ give 0.069271 instead of 0.255326. These inputs are illustrative and are not a computed Yang–Mills beta function. Wave-function factors, mixing and strong-coupling evolution would have to be supplied by a full calculation.

3 Why local stiffness does not establish a bulk gap

3.1 The derivative control

For a free transverse polarisation at the trivial background, a positive dimension-six derivative term gives a quadratic kernel of the form $K(p) = \hat{p}^2 + \lambda_6(\hat{p}^2)^2$, with fixed finite $\lambda_6 \geq 0$. On a periodic unit lattice, excluding the constant mode,

$$\hat{p}^2_{\min} = 4\sin^2(\pi/L), \qquad K_{\min}(L) = 4\sin^2(\pi/L) + 16\lambda_6 \sin^4(\pi/L) \to 0.$$

The same conclusion follows from smooth normalised wave packets of extent R: their quadratic cost is of order $R^{-2} + \lambda_6 R^{-4}$. A block Poincaré estimate can be correct with fixed block boundaries while the assembled system regains arbitrarily soft collective modes. This is an obstruction to the proposed derivative-only Hessian argument; it is not a proof that interacting quantum Yang–Mills is gapless.

3.2 Positive density and rare empty regions

Proposition 3.1. Translation invariance, ergodicity, mixing and a positive density of sites with positive potential do not imply a positive lower spectral edge for a random Schrödinger operator. **Proof.** Consider independent site potentials taking values zero and one, both with positive probability. For any fixed cube size n, an all-zero cube has positive probability. Infinitely many disjoint trials imply that such cubes occur almost surely. Taking the countable intersection over n gives arbitrarily large zero-potential cubes. A Dirichlet test function supported in one has Rayleigh quotient

$$\lambda_D(n) = 4d\sin^2\left(\frac{\pi}{2(n+1)}\right) \to 0.$$

The potential is nonnegative, so the spectral infimum is zero. The ensemble is independent and hence strongly mixing, while the positive-potential density is nonzero. A continuum version follows from independent piecewise-constant potentials on unit cubes. The missing step in the old covering argument was replacing a positive spatial fraction by a lower bound on the fraction of the norm of every test function lying there; test functions can concentrate in the large empty regions.

3.3 The oscillation estimate and threshold algebra

The companion paper also used a bound of the maximum oscillation on a four-dimensional cube by the mean absolute gradient. That bound is false without additional regularity. Let $f_\delta(x) = \max(1 - |x|/\delta, 0)$, supported inside the unit four-cube. Then

$$\operatorname{osc} f_\delta = 1, \qquad \int |\nabla f_\delta| \, d^4x = \frac{\pi^2}{2}\delta^3 \to 0.$$

The valid elementary Lipschitz bound uses $\operatorname{diam}(B) \parallel \nabla f \parallel_\infty$. An averaged Sobolev bound strong enough to control oscillation requires the appropriate higher integrability, for example a Morrey estimate with exponent greater than four. Ratios whose numerator and denominator both scale as κ^2 also do not acquire an automatic κ^2 suppression after averaging.

A separate correction concerns the coupling count in local thresholds. If $Q_0 \geq -m_{\text{base}} \parallel \psi \parallel^2$, the uncoupled higher-derivative form satisfies $\overline{Q}_6 \geq c \parallel \psi \parallel^2$, and the remainder is at most $\lambda_6 e \parallel \psi \parallel^2$, then

$$Q_0 + \lambda_6 \overline{Q}_6 - E_{\text{rem}} \geq [\lambda_6(c - e) - m_{\text{base}}] \parallel \psi \parallel^2.$$

For $c > e$, the sufficient linear threshold is $\lambda_6 \geq \left(m_{\text{base}} + m_{\text{target}}\right)/(c - e)$. A quadratic threshold belongs to a different action with a genuinely quadratic coupling dependence. Correcting this arithmetic does not supply the missing global coercivity assumption.

4 What exact coarse graining preserves

4.1 Temporal blocking and physical energy

Theorem 4.1. Let T be a positive self-adjoint transfer operator, normalised to have vacuum eigenvalue one. Retaining complete spatial slices every b time steps gives the exact transfer T^b. If r is a nonvacuum spectral value and a_t is the original time step, its physical energy is unchanged:

$$E = -\frac{\log r}{a_t} = -\frac{\log\left(r^b\right)}{b a_t}.$$

Proof. Apply spectral calculus to T^b. If the nonvacuum spectrum accumulates at one, its powers also accumulate at one. Thus exact temporal blocking preserves an existing gap and cannot create one from a gapless transfer. Spatial coarse graining can remove overlap with low states in selected observables; an apparent increase in a measured gap must therefore be distinguished from a change in the full physical spectrum.

4.2 Gaussian and compact group controls

Exact integration of Gaussian eliminated variables gives the Schur complement $K_{\mathrm{eff}} = K_{BB} - K_{BF}K_{FF}^{-1}K_{FB}$. In the periodic derivative control it preserves the constant null vector, and the nonconstant soft modes survive. Four-dimensional point decimation gives the covariance alias sum

$$G_b(q) = b^{-4} \sum_{r\in\{0,\dots,b-1\}^4} \frac{1}{K\big((q+2\pi r)/b\big)}, \qquad K_b(q) = G_b(q)^{-1}.$$

The soft alias forces the retained kernel to vanish at small momentum when the retained observable has nonzero overlap with it. One-dimensional real-space Schur complements and four-dimensional alias sums verify this directly. A small mass regulator can be used to define inverses before taking the massless limit.

A nonlinear compact-group control is the SU(2) rotor chain with normalised convolution kernel proportional to $\exp[(\beta/2)\mathrm{tr}(UV^{-1})]$. Character orthogonality, with Haar density $(2/\pi)\sin^2\theta\, d\theta$ for class functions, yields the spin-j transfer eigenvalue

$$r_j(\beta) = \frac{I_{2j+1}(\beta)}{I_1(\beta)}.$$

Direct Haar quadrature verifies the Bessel formula. At $\beta = 2$ the first rotor energy is 0.83672331 per original time unit for block factors 1, 2, 4 and 8. Fitting a single Wilson-form coupling after a two-step block matches the fundamental channel but overestimates the adjoint eigenvalue by 32.73 percent. The exact blocked character expansion is not generally a one-parameter family. This rotor is not four-dimensional Yang–Mills and its first excitation is not a glueball.

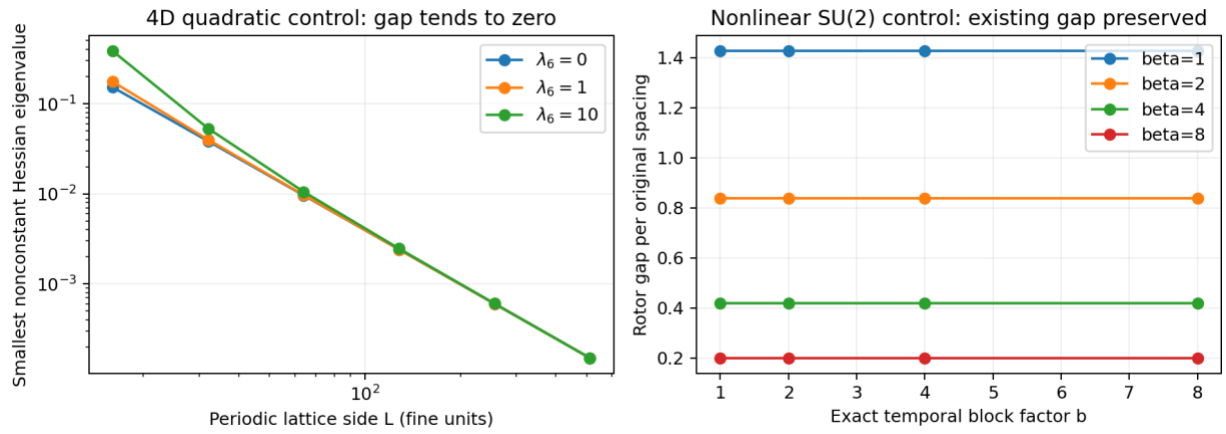


Figure 1. The derivative control remains soft as the periodic side grows. Exact temporal blocking preserves the physical gap of the separate SU(2) rotor control. Neither calculation is an interacting four-dimensional gauge-field simulation.

Positivity of a Boltzmann weight is not by itself reflection positivity. A truncated fourth-order Euclidean kernel, in particular, is not automatically a fundamental unitary relativistic theory. Likewise, a finite-range blocking map need not yield an exactly finite-range effective action. A physical application must preserve the complete pushforward measure or control its discarded interactions and reflection structure.

4.3 Exact protection of the complete retained response

The later corpus supplies a stronger positive result than preservation of a few selected observables [17, §§33–37]. Let a finite fine catalogue Y map to retained labels X. Let S_f be a row-stochastic transition with

strictly positive stationary law μ, and let π be its marginal on X. Write $D_\mu = \mathrm{diag}(\mu)$ and similarly for D_π. The lift and conditional average satisfy

$$(Lg)_a = g_{p(a)}, \qquad \mathcal{C} = D_\pi^{-1} L^T D_\mu, \qquad \mathcal{C}L = I, \qquad L^T D_\mu L = D_\pi.$$

Assume the fine law is reversible and obeys the exact grouping identity $S_f L = L T_0$. This condition says that the probability of reaching any retained label does not depend on which internal description of the departure label was used. Set $Q_f = D_\mu(I - S_f)$ and $Q_0 = D_\pi(I - T_0)$.

Theorem 4.2. Under these hypotheses, for every retained value g,

$$\min_{\mathcal{C}f = g} f^T Q_f f = g^T Q_0 g.$$

Proof. Write $f = Lg + f_\perp$, where $\mathcal{C}f_\perp = 0$. Grouping gives $(I - S_f)L = L(I - T_0)$, and reversibility makes Q_f symmetric positive semidefinite. Thus the cross term vanishes and

$$f^T Q_f f = g^T Q_0 g + f_\perp^T Q_f f_\perp.$$

Taking $f_\perp = 0$ attains the lower bound. This preserves the complete retained quadratic form, including every retained contrast response; no independence of the internal variables is required. The equality holds at every level of a family satisfying the hypotheses in one normalization. The exact source theorem therefore extends beyond its finite numerical examples.

The grouping and reversibility conditions are physical requirements when this theorem is applied to a source. The canonical reversible catalogue and the driven FCHI/PFDMI history law are different. In the nonreversible case, simultaneous preservation by the forward transition and its stationary adjoint is a sufficient extension. Forward grouping alone can change the minimized symmetric response [17, §36].

Lemma 4.3 (retained and hidden spectral decomposition). Equip fine and retained observables with the stationary inner products $\langle f, g\rangle_\mu = f^T D_\mu g$ and $\langle u, v\rangle_\pi = u^T D_\pi v$. Under Theorem 4.2, L is an isometry, $\mathcal{C} = L^*$, and $P = L\mathcal{C}$ is the orthogonal projector onto $\mathrm{ran}L$. Both $\mathrm{ran}L$ and $\ker\mathcal{C}$ reduce S_f. In particular,

$$\mathcal{C}S_f = T_0\mathcal{C}, \qquad PS_f = S_f P, \qquad I - S_f \simeq (I - T_0) \oplus G_{\mathrm{hid}}, \quad G_{\mathrm{hid}} = (I - S_f)|_{\ker\mathcal{C}}.$$

Proof. Take the weighted adjoint of $S_f L = L T_0$. Reversibility of S_f induces reversibility of T_0 and gives $\mathcal{C}S_f = T_0\mathcal{C}$. Thus $\ker\mathcal{C}$ is invariant and is orthogonal to the invariant lifted space. Restricting to the two spaces gives the unitary direct sum. The finite spectrum, including multiplicities, is the union of the retained and hidden spectra. If the fine chain is irreducible, its constant mode lies in the retained space and

$$\gamma_f = \min\{\gamma_0, \inf\sigma(G_{\mathrm{hid}})\}.$$

The grouping hypothesis determines the retained block but imposes no refinement-uniform positive lower bound on the hidden block. Stochastic positivity and reversibility still constrain which hidden blocks are admissible. This is a statement about the weighted relaxation generator $I - S_f$, not the ordinary Euclidean eigenvalues of the Dirichlet matrix Q_f or a quantum mass. No tensor-product assumption is involved.

4.4 A preserved retained response with a vanishing fine gap

Proposition 4.4. The hypotheses of Theorem 4.2 alone do not imply a uniform spectral gap for the full fine relaxation operator. **Construction.** Use the canonical seven-address transition from [17]: its hub row has seven entries $1/7$, while a rim row has entries $1/4$ on the hub, itself and its two rim neighbours. Its

stationary law is $\pi = (7,4,4,4,4,4,4)/31$, and its nonconstant relaxation gap is $1/2$. Let R_n be the symmetric nearest-neighbour transition on an internal cycle with $n \geq 3$ vertices. Define

$$S_n = T_0 \otimes I_n + \frac{1}{8} I_7 \otimes (R_n - I_n), \qquad \mu_n = \pi \otimes \frac{\mathbf{1}_n}{n}.$$

Every entry is nonnegative because the smallest diagonal of T_0 is $1/7 > 1/8$. The transition is stochastic and reversible. Lifting a retained observable constantly over each internal cycle gives $S_n L = L T_0$, so Theorem 4.2 applies exactly. The two tensor factors commute. Their eigenvalues show that the lowest nonzero eigenvalue of $I - S_n$ is

$$\gamma_n = \frac{1}{8}\left[1 - \cos\left(\frac{2\pi}{n}\right)\right] \to 0.$$

The corresponding mean-zero internal mode is invisible to $\mathcal{C}$. Hence every retained response can stay fixed while this unresolved motion becomes arbitrarily slow. This is an analytic sequence, not an extrapolation from the following finite checks.

Internal cycle n	Fine states	Retained relaxation gap	Full relaxation gap
3	21	0.500000	0.187500000
4	28	0.500000	0.125000000
8	56	0.500000	0.036611652
16	112	0.500000	0.009515058
32	224	0.500000	0.002401840

All 21 retained pair responses agree at each size; their minimum remains $279/20 = 13.95$. Their maximum numerical discrepancy is 4.98×10^{-14}. This pair-response value is an inverse-Dirichlet diagnostic, not an energy. Likewise, γ_n is a relaxation gap, not a Yang–Mills mass. The added cycles are constructed controls whose physical admission in VERSF has not been asserted. The result identifies the missing inference: an actual physical refinement must either remove such hidden modes as redundancies or provide uniform energetic control of them.

A second construction couples the hidden transition to the retained endpoints. Label the fine states (x, s) with $s = \pm 1$, and set $\beta_{xy} = 1 + [(x + y) \bmod 4]/4$ for $x, y = 0, \ldots, 6$. For $0 < \varepsilon \leq 0.1$, let

$$S_\varepsilon\big((x,s),(y,t)\big) = T_{0,xy}\left[\left(1 - \varepsilon\beta_{xy}\right)\mathbf{1}_{t=s} + \varepsilon\beta_{xy}\mathbf{1}_{t=-s}\right].$$

This chain is irreducible and reversible for $\mu_{x,s} = \pi_x/2$, and it obeys exact grouping. Its hidden sign-flip probability depends on both endpoints, so it is not a retained-independent tensor transition. The odd sector is represented by the matrix with entries $T_{0,xy}\left(1 - 2\varepsilon\beta_{xy}\right)$. The unit-norm trial observable $f(x,s) = s$ gives

$$0 < \gamma_f \leq 2\varepsilon \sum_{x,y} \pi_x \, T_{0,xy}\beta_{xy} \to 0.$$

The full gaps at $\varepsilon = 0.1, 0.01, 0.001, 0.0001$ are approximately $0.283069, 0.0283814, 0.00283865, 0.000283870$, while the retained gap stays $1/2$. Lemma 4.3 explains

the invariant spectral splitting in both examples; it is imposed by exact reversible grouping even when the microscopic transitions are not a product.

Effect of a continuation-faithful quotient. If the admissible future channel consists only of the retained-label process, exact grouping makes every future retained-path probability independent of s (or of the cycle label in the first example). Those labels are then continuation-invisible and the maximal faithful quotient removes them. Their small gaps are not physical excitations of that quotient. If additional admissible observations or interventions distinguish them, the relevant continuation channel is larger and its surviving hidden sector needs a bound. Reference [22, §§7.1–7.3] defines faithfulness relative to a specified channel; it does not identify that channel with every microscopic coordinate. The examples therefore refute an inference about the unquotiented fine spectrum, not the continuation-faithful construction itself.

4.5 A uniform fibre gap controls the hidden sector

Let $F_x = p^{-1}(x)$ be a fibre and $\mu_x(a) = \mu_a/\pi_x$ its conditional stationary law. Under Theorem 4.2, retain the original within-fibre rates $S_f(a,b)$ for distinct $a, b \in F_x$ and turn every exit from F_x into holding. This defines a reversible stochastic kernel on F_x. Its Poincaré constant κ_x is the largest number satisfying

$$\mathcal{E}_x(g) = \frac{1}{2}\sum_{a,b\in F_x} \mu_x(a) S_f(a,b)|g(a) - g(b)|^2 \geq \kappa_x \mathrm{Var}_{\mu_x}(g).$$

Proposition 4.5 (uniform fibre control). For a finite irreducible reversible chain obeying exact grouping, write γ_0 for the retained relaxation gap, $\gamma_{\mathrm{hid}} = \inf\sigma(G_{\mathrm{hid}})$ and $\kappa_* = \min_x \kappa_x$. Then

$$\gamma_f = \min\{\gamma_0, \gamma_{\mathrm{hid}}\}, \qquad \gamma_{\mathrm{hid}} \geq \kappa_*, \qquad \gamma_f \geq \min\{\gamma_0, \kappa_*\}.$$

Proof. The equality is Lemma 4.3. If $f \in \ker\mathcal{C}$, every conditional mean is zero. Drop the nonnegative cross-fibre terms in the fine Dirichlet form and apply each fibre inequality:

$$\langle f, (I - S_f)f\rangle_\mu \geq \sum_x \pi_x \mathcal{E}_x(f|_{F_x}) \geq \sum_x \pi_x \kappa_x \| f \|^2_{\mu_x} \geq \kappa_* \| f \|^2_\mu.$$

Taking the infimum over hidden unit vectors proves the bound. A singleton fibre has no mean-zero subspace and can be assigned $\kappa_x = +\infty$; if the entire hidden sector is absent, the full gap equals the retained gap. The same argument gives a uniform family bound when both the retained gap and all nontrivial fibre constants have uniform positive floors.

This is a sufficient, checkable source condition, not a necessary condition. Cross-fibre motion can mix hidden variables even when the within-fibre constants vanish. Nor may one replace these kernels by transitions conditioned on staying in a fibre without restoring the omitted holding factor: that changes the clock and can conceal slow internal relaxation. For a source step of physical duration τ, the generator relaxation rates are γ/τ and κ/τ. A quantum energy requires the additional transfer identification of Section 4.1.

An independent seeded test on 300 reversible exactly lumpable chains verifies the full spectral union, the minimum-gap identity and the fibre lower bound. The microscopic cross-fibre transitions depend on both endpoints and are not assumed to be a product. The tests include varying catalogue sizes and nonuniform retained stationary laws. They check the implementation; the Dirichlet-form proof supplies the result for all chains satisfying the hypotheses.

5 Information balance and exact commitment constraints

5.1 An exact information identity

A controlled recording isometry maps a pure system superposition and blank pointer to $|\Psi\rangle = \sqrt{p}\,|0\rangle|r_0\rangle + \sqrt{1-p}\,|1\rangle|r_1\rangle$. Let C_z be relative-entropy coherence of the reduced system in the recorded basis, and χ_R the Holevo information of the pointer ensemble. The conditional pointer states are pure. Using standard coherence definitions [10] and the equality of the two marginal entropies,

$$C_z = H_2(p) - S(\rho_S), \qquad \chi_R = S(\rho_R), \qquad C_z + \chi_R = H_2(p).$$

Thus lost local coherence can be balanced exactly by gained record information. The global state remains pure, with phase information stored in correlations. At partial recording, Holevo information is an upper bound on accessible classical information; the quantum mutual information of this pure bipartite state is $2S(\rho_R)$. These quantities must not be added as interchangeable information counts. The model is a reversible premeasurement control, not a derivation of irreversible fact commitment [11].

An information amount alone does not fix an energy scale. With $\hbar = 1$, the Hamiltonian $H_\eta = \eta|1\rangle\langle 1| \otimes (I - X)/2$ makes a perfect one-bit record from the relevant initial state in time π/η. Its bandwidth can be arbitrarily small if the process takes correspondingly longer. Fixed completion time, durability and reset conditions would add separate physical requirements.

5.2 The selected primitive carrier and allowed operations

PMS-EX58 derives the primitive binary carrier, its selected projectors, completion and branch-preserving renewal relative to the primitive fact-commitment axiom [4, §§28–29]. We retain that result. The present question concerns the excitation spectrum after that selection, rather than repeating the primitive carrier derivation. The distinct map from those records to continuous field and current coordinates must retain its own source status.

The exact preservation criterion in SGW-2 [5, §13.2], linked there to the post-commitment operation [7], makes the excluded motions precise. Let $\{P_r\}$ be a complete orthogonal sharp-record partition and $\mathcal{E}(\rho) = \sum_\alpha K_\alpha \rho K_\alpha^\dagger$ a trace-preserving channel. Then

$$\mathcal{E}^\dagger(P_r) = P_r \;\forall r \quad \Leftrightarrow \quad P_s K_\alpha P_r = 0 \text{ for } s \neq r \quad \Leftrightarrow \quad K_\alpha = \sum_r P_r\, K_\alpha P_r.$$

Proposition 5.1. These equivalences hold exactly. **Proof.** For a vector in the range of P_r and $s \neq r$, preservation makes the sum $\sum_\alpha \| P_s K_\alpha \psi \|^2$ zero. Each nonnegative term vanishes. Conversely, block-diagonal Kraus operators and trace preservation imply the adjoint identities. For a unitary flow generated by A, the condition is $[A, P_r] = 0$. Enlarging the record carrier under renewal requires the corresponding input-output intertwining relation.

For $P_\pm = (I \pm \sigma_z)/2$, the off-diagonal generator components σ_x and σ_y are excluded, while I and σ_z remain. However, a record sector may contain working degrees of freedom: an operator $I_{\text{ledger}} \otimes A_{\text{work}}$ preserves every ledger projector. This proves compatibility with record retention, not selection of arbitrary independent working motions.

The source explicitly distinguishes a binary rephasing from an independent MASD/HX1 polar phase. Its separate-ledger append construction has identically zero old-history leakage derivatives on working parameters [5, §13.5]; those zero rows are not the full physical record constraint. For an actual continuation map, stack the derivatives of forbidden leakage amplitudes into J_{rec} and intersect its kernel

with the admitted tangent space. First derivatives of transition probabilities alone can miss forbidden directions because probabilities begin quadratically in the leakage amplitude.

5.3 What the native record and renewal results preserve

The marked-anchor and later Fold papers recover source-native sharp departure-address effects [18, §23B; 17, §31]. For the declared history operators $H_{y\leftarrow x} = \sqrt{T_{xy}}|y\rangle\langle x|$, completeness gives

$$\sum_y H_{y\leftarrow x}^\dagger H_{y\leftarrow x} = P_x, \qquad P_x = |x\rangle\langle x|.$$

Complete internal refinement retains $P_x \otimes I$. These are records of the departure address. They are not automatically a physical position, a Fold-presence projector or a present matter–record phase reference. Each P_x commutes with every diagonal site rephasing, so address probabilities alone cannot fix those phases. That observation is at the effect level: it neither proves preservation of coherence by the full channel nor establishes that an independent continuous phase survives commitment.

The continuation-faithful coarse-graining theorem protects distinctions that change the specified admissible future channel [22, §§7.1–7.3]. It also permits removal of distinctions that do not change that channel. Thus the hidden labels of Section 4.4 disappear if the retained-label process exhausts the admissible continuation content. A physical application must identify the complete channel and its carrier before counting hidden states as excitations. For the rank-one trap construction, the marked-anchor source states the stronger physical identity

$$\sum_\alpha K_\alpha^\dagger Q_h K_\alpha = I - \Pi_{\mathrm{adm}}(h).$$

Availability of rank-one projectors in an operator algebra is not that identity. The topological forbidden direction, the chosen history-dependent projector and the actual physical instrument must be identified on one carrier. The later PMS ledger retains this distinction as D-PM40 and D-PM41, while treating fact production itself as the primitive FC axiom [4]. The existence of a fact is therefore not reopened as a missing pre-fact dynamical derivation.

There is also a positive same-action result directly relevant to stiffness. The post-commitment paper identifies the HX1 variable with the phase tangent of the polar part of the master record/completion morphism Φ [7, §46R]. In the declared unit uniform-cycle block,

$$H_{qy} = \begin{pmatrix} 3 & -1 \\ -1 & 2 \end{pmatrix}, \qquad k_{\mathrm{relaxed}} = 3 - \frac{1}{2} = \frac{5}{2}, \qquad k_{\mathrm{locked}} = 3.$$

The minimal branch-preserving renewal cannot regenerate this continuous phase: its free phase cancels from both renewed link ratios and the conditioned density state. Thus loss of this old relaxation direction cannot be undone by that minimal renewal. The remaining local question is whether the complete commitment morphism actually removes the old HX1 tangent. Discrete record retention alone does not settle that question. The cycle calculation and its physical operational normalization must also be distinguished from the full spatial relative-phase constraint of Section 8.

6 Why a live record can preserve a soft mode

A scalar control separates a mismatch cost from a restriction on allowed motion. Give a field x and record coordinate r canonical kinetics, equal gradient terms and potential $\kappa(x-r)^2/2+\mu^2 r^2/2$. At squared spatial momentum q the stiffness is

$$K(q)=\begin{pmatrix} q+\kappa & -\kappa \\ -\kappa & q+\kappa+\mu^2 \end{pmatrix}.$$

When $\mu=0$, its eigenvalues are q and $q+2\kappa$. The relative motion is costly, while common motion remains soft. Integrating out the live record gives a subtractive response, not the result of freezing it:

$$K_{\text{eff}}(q)=q+\kappa-\frac{\kappa^2}{q+\kappa+\mu^2}.$$

This is a static precision; temporal response must also be retained before interpreting it as an energy. At $\mu=0$, its limit is zero. A nonlinear mismatch $V(x-r)$ does not remove the common mode in this particular model: the orthogonal variables $(x+r)/\sqrt{2}$ and $(x-r)/\sqrt{2}$ separate a free common field from the interacting relative field. This is an exact action-level statement for equal canonical kinetic and gradient coefficients, not a universal claim about nonlinear records.

The local integral $Z(x)=\int e^{-V(x-r)}dr$ is independent of x. Consequently its marginal curvature vanishes by $\langle V''\rangle-\mathrm{Var}(V')=0$, consistent with Proposition 2.2. A fixed record, a restoring interaction and a live marginalised record are different physical constructions.

Strict preservation must also be separated from a small transition rate. For the oscillator-memory control $H=p_x^2/2+(x-Z)^2/2-\delta X$, each fixed-$Z$ sector has gap one when $\delta=0$. When memory flips are permitted, the low doublet splits by approximately $2\delta e^{-1}$ and becomes arbitrarily soft as $\delta\to 0$. The exact zero-flip model has two vacuum sectors. Neither a sector gap nor long memory lifetime by itself establishes a unique-vacuum gap for the full system.

7 The published spatial field, current and record action

We now use the explicit spatial action of Source History Weighting [6, §19.5, Eq. (154)], rather than identifying the finite internal wheel spectrum with spatial momentum. Its variables are a link phase θ, current u, polar-record phase y, matter phase ϕ and completion coordinate η. Write $d_i=2\sin(p_i/2)$, $\mathcal{R}=i[d\times]$ and $q=d^{\dagger}d$. With all listed weights positive,

$$2S=a\parallel \mathcal{R}\theta\parallel^2+w_J\parallel u+\theta-d\phi\parallel^2+w_T\parallel d^{\dagger}u\parallel^2$$

$$+b\parallel \mathcal{R}y\parallel^2+c\parallel \theta-y\parallel^2+(w_H+m)|\eta|^2.$$

The declared gauge direction is $(d,0,d,1,0)$. Fixing $\phi=0$ leaves ten complex Fourier coordinates, with opposite momenta related by the reality condition. The benchmark takes $a=b=c=w_J=w_T=1$ and $w_H+m=2$, with identity kinetic metric. The action is a bosonic phase restriction: radial matter, the separate fermion correction, nonlinear interactions and the complete physical record pullback are not included. The source does not identify this finite spatial complex or its reference history potential with the complete physical source [6, §§19.5, 19.7].

The two transverse polarisations each have the first block below; the longitudinal sector has the second. Within each block the coordinates are (θ, u, y). Completion contributes eigenvalue two.

$$K_T(q) = \begin{pmatrix} q+2 & 1 & -1 \\ 1 & 1 & 0 \\ -1 & 0 & q+1 \end{pmatrix}, \qquad K_L(q) = \begin{pmatrix} 2 & 1 & -1 \\ 1 & 1+q & 0 \\ -1 & 0 & 1 \end{pmatrix}.$$

Theorem 7.1. The unconstrained unit parent has arbitrarily soft nonzero-momentum modes as the periodic side grows. **Proof.** Take $v = (1, -1, 1)^T$. Both mismatch terms vanish along this coordinated motion. Its exact Rayleigh quotients are

$$\frac{v^T K_T v}{v^T v} = \frac{2q}{3}, \qquad \frac{v^T K_L v}{v^T v} = \frac{q}{3}.$$

For $q > 0$ the blocks are positive definite. At zero momentum each has one null direction v. Perturbation gives the lowest eigenvalues $2q/3 + O(q^2)$ and $q/3 + O(q^2)$. Since the smallest nonzero q is $4\sin^2(\pi/L)$, no uniform positive frequency floor exists in this family. The argument does not rely on retaining the exactly constant mode.

The witnesses are not gauge directions of the declared parent: transverse motion has nonzero curvature $\mathcal{R}\delta\theta$, and the longitudinal witness has nonzero gauge-invariant current δu. For a longitudinal vector parallel to d, $\mathcal{R}\delta y = 0$, so fixing every spatial record-loop phase leaves this soft branch. Its admission under the complete physical Gauss law, source constraints and pure non-Abelian sector has not been established. It therefore identifies a gap in the restricted-model argument rather than a physical Yang–Mills counterexample.

For arbitrary fixed positive weights the same trial-vector numerators are $(a + b)q$ transversely and $w_T q$ longitudinally. An inertia bounded above and bounded away from zero preserves the soft scaling. Changing finite local coefficients alone does not remove the coordinated direction.

Periodic side L	Free transverse frequency	Loop-locked joint frequency	Full relative-phase lock
16	0.311536	0.215926	0.649642
64	0.080020	0.056507	0.620177
256	0.020038	0.014168	0.618169
1024	0.005010	0.003543	0.618042

These are normal-mode frequencies in the unit model. The full relative-phase column refers to the additional constraint introduced next. The finite internal cycle eigenvalues $\{1,2,2,4,4,5\}$ instead give minimum frequency 0.684040287 in their separate unit calculation; that finite-carrier result does not establish a spatial bulk gap.

7.1 An explicit test of every closed loop

The complete-loop calculation makes the loop statement independent of a local plaquette approximation. On a connected periodic cubic graph with $V = N^3$ vertices and $E = 3V$ edges, let D be the vertex-to-edge difference map and let B_{cyc} stack all plaquettes and the three independent winding cycles. The full closed-cycle space has dimension $E - V + 1$. Hence

$$B_{\mathrm{cyc}}D = 0, \qquad \ker B_{\mathrm{cyc}} = \mathrm{range}(D), \qquad \dim\left(\ker B_{\mathrm{cyc}}\right) = V - 1.$$

Every exact gradient therefore preserves all closed-loop phases, including winding records. For $y \mapsto y + tD\eta$, the Abelian phases $\exp\left(iB_{\mathrm{cyc}}y\right)$ are unchanged at every real t. Along $(\delta\theta, \delta u, \delta y) = (D\eta, -D\eta, D\eta)$ the two mismatch costs vanish and only the current-divergence cost remains. Root-to-vertex open-path records would supply the missing $V - 1$ independent conditions, but their physical commitment is an additional requirement. Explicit ranks were verified for $N = 2,3,4$, and full constrained real-space spectra for $N = 2,3$. Flat SU(2) link products also telescope around loops; that is a record-geometry check, not an interacting non-Abelian spectral calculation.

Imposing both complete loop locking and the extra hard condition $D^{\dagger}u = 0$ removes this longitudinal witness in the unit parent and recovers the same positive benchmark as full relative-phase locking. This is only a sufficient mathematical comparison. Physical continuity relates current divergence to changing matter density, so replacing it by zero can forbid legitimate compensated motion. Appendix B.1 derives this distinction directly from continuity. Neither the hard divergence condition nor complete open-path commitment is inferred from closed-loop retention alone.

7.2 The native neutral reference and physical admission

The representation-valued master current makes the physical-admission qualification concrete [20, §42; 17, §§19–21; 23, §65]. Its endpoint and current are vectors in $\mathbb{C}^{50}$, with constitutive residual

$$D_{J,e} = j_e - \left(\psi_{t(e)} - U_e\psi_{s(e)}\right).$$

The native neutral reference ν_0 is annihilated by all twelve generators. Consequently a pure gauge link family obeys

$$T_a\nu_0 = 0, \qquad U_e = g_{t(e)}g_{s(e)}^{\dagger}, \qquad U_e\nu_0 = \nu_0.$$

For $\psi_v = \nu_0$, $j_e = 0$ and record transport $V_e = U_e$, this flat family is a gauge transform of the corresponding trivial-link configuration. The endpoint difference vanishes. In particular, the scalar unit-current coupling of the restricted parent is not automatically the coupling obtained by linearizing this native neutral reference. The current response to a pure link variation vanishes there, as the source-kernel analysis states [20, §42].

The archived generator arrays verify $T_a\nu_0 = 0$ for all twelve generators and the finite endpoint identities on all twelve wheel edges. With a fixed charged test ray χ, the same links can give $j_e = \chi - U_e\chi \neq 0$; with the co-moving ray $\psi_v = g_v\chi$, the covariant difference is zero. Holding the reference fixed and transporting it jointly are different physical prescriptions. Neither test selects the physical quantum vacuum or excludes neutral composite excitations.

Theorem 7.1 and Proposition 9.3 therefore remain exact for their declared scalar parent, but are not gapless-state theorems for the complete VERSF or pure Yang–Mills theory. Their use requires an embedding of the trial direction in the actual physical tangent space, after the complete Gauss constraints

and gauge quotient. If the source excludes that direction already, an additional phase-locking mechanism is unnecessary for that direction; the remaining physical modes still require their own energy bound.

7.3 Different comparison spaces require different tests

On the seven-vertex wheel, the vertex-to-edge incidence D has rank six and the six independent cycle rows B_{cyc} also have rank six, with $B_{\mathrm{cyc}}D = 0$. The cut and cycle subspaces are orthogonal and together exhaust the twelve-dimensional edge space. These six spatial cut directions are different from the RCHS rank-six current carrier, which consists of the three colour, weak and hypercharge factors resolved over two cycle quadratures [19, §39A]. Rank agreement does not identify their observables or constraints.

A closed comparison of two paths with the same endpoints cannot distinguish a common flat endpoint transport. If both link and record transport have the form $U_e = V_e = g_t g_s^{\dagger}$, every path product telescopes to $g_{\mathrm{end}} g_{\mathrm{start}}^{\dagger}$, and the two-route difference is zero. This exact statement includes the balanced co-terminal comparator of [18, §23N]. It does not decide whether a separately prepared matter reference is fixed, transported or itself altered by commitment.

To test a proposed comparison constraint, its source operation must specify the preparation, both comparison routes, the retained outcome and the evolution of any reference. Differentiate those complete conditions, including a moving reference where applicable. A nonzero sensitivity with other variables frozen is not an exact preservation condition on the jointly responding system. The native on-shell probability-rank calculation supplies a response theorem at its tested backgrounds [23, §§67–69]; it does not by itself supply the required forbidden-motion projector.

8 Abelian phase pinning and conditional gaps

8.1 Hard locking and the Stueckelberg mass term

Impose the additional linearised constraint $y - d\phi = 0$, which is gauge invariant under the declared parent gauge direction. In the gauge $\phi = 0$, this sets $y = 0$. It fixes every relative record phase, not only its curl. We restrict the configuration variables and their induced canonical dynamics before quantisation. This is not the claim that projecting a live quantum coordinate onto an exact position eigenstate has finite energy.

This constraint exposes a familiar mechanism: the mismatch term becomes $c \parallel \theta - d\phi \parallel^2/2$, an Abelian Stueckelberg-type mass term [24]. The gauge-invariant field is $A = \theta - d\phi$; in the gauge $\phi = 0$ the term has the Proca form $c \parallel \theta \parallel^2/2$. The independent relative record phase is frozen. The gapped object is a massive Abelian phase field coupled to the stated Gaussian current and completion coordinates. The construction is not a non-Abelian mass-generation mechanism.

$$\frac{a}{2} \parallel \mathcal{R}A \parallel^2 + \frac{c}{2} \parallel A \parallel^2 = \frac{1}{2} \parallel \mathcal{R}A_{\mathrm{can}} \parallel^2 + \frac{m_{\mathrm{S}}^2}{2} \parallel A_{\mathrm{can}} \parallel^2, \qquad A_{\mathrm{can}} = \sqrt{a}\, A, \quad m_{\mathrm{S}}^2 = \frac{c}{a}.$$

The fixed physical ratio c/a supplies a spatial inverse-length-squared scale. It becomes the usual relativistic mass squared only after the matching temporal normalization is established. For $\hbar = 1$, an algebraic current and field inertia m_θ give zero-momentum energy squared $\omega^2 = c/m_\theta$. A dynamical current changes that eigenvalue further. The present model supplies c, a and the kinetic coefficients as inputs. Its dynamics does not generate or select this mass scale. The full auxiliary-field model has not been identified with relativistic Proca theory, let alone pure Yang–Mills theory.

Theorem 8.1 (hard-locked Abelian Gaussian gap). In the unit quadratic model with this full constraint and identity kinetic metric, every retained normal mode has squared frequency at least $\mu_0 = (3-\sqrt{5})/2$.

Proof. The reduced blocks are

$$K_{T,\mathrm{lock}}(q) = \begin{pmatrix} q+2 & 1 \\ 1 & 1 \end{pmatrix}, \qquad K_{L,\mathrm{lock}}(q) = \begin{pmatrix} 2 & 1 \\ 1 & q+1 \end{pmatrix}.$$

$$A_0 = \begin{pmatrix} 2 & 1 \\ 1 & 1 \end{pmatrix}, \qquad K_{T,\mathrm{lock}} \succcurlyeq A_0, \quad K_{L,\mathrm{lock}} \succcurlyeq A_0, \quad \lambda_{\min}(A_0) = \mu_0 > 0.$$

Each block differs from A_0 by a positive semidefinite gradient term; completion has stiffness two. Taking square roots gives the frequency floor $\sqrt{\mu_0} = 0.618034$. Equality occurs at zero momentum and is approached by nonzero momenta as the volume grows. No finite-cell boundary estimate is needed.

For general positive local coefficients $w = w_J$ and c, the onsite matrix is $A(w,c) = \begin{pmatrix} w+c & w \\ w & w \end{pmatrix}$, with determinant wc and lower eigenvalue

$$\alpha(w,c) = \frac{2w + c - \sqrt{c^2 + 4w^2}}{2} > 0.$$

With nonnegative gradient terms, completion stiffness $m_\eta^2 > 0$ and a positive quadratic inertia satisfying $M \preccurlyeq M_{\max} I$, a sufficient squared-frequency bound is $\min\{\alpha(w,c), m_\eta^2\}/M_{\max}$. Uniformity of this ratio is the substantive requirement when the coefficients depend on a regulator or background.

The theorem is conditional on the full constraint. Exact retention of a sharp fact label does not imply that every independent continuous record phase is fixed. The protected-holonomy restriction in SGW-2 [5, §17] and the master-phase/minimal-renewal result of Section 5.3 retain their cycle-mode scope. Neither implies the full spatial relative-phase lock. Alternatively, the actual physical quotient may exclude the candidate direction, or additional derived interactions may lift it. The native neutral example in Section 7.2 shows why the physical carrier must be identified before choosing among these possibilities.

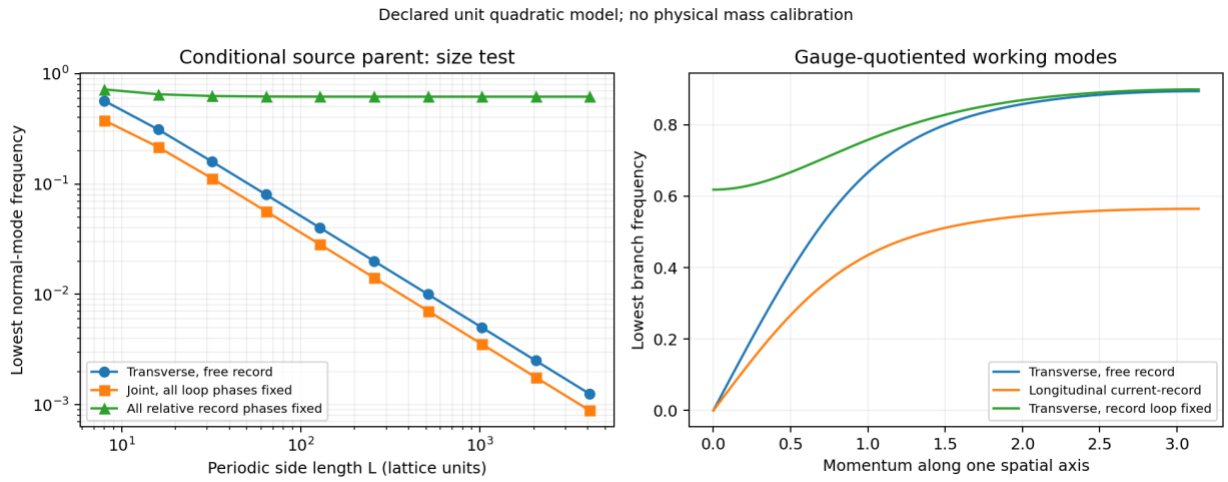


Figure 2. The published unit spatial parent contains soft joint modes. Fixing loop phases removes the transverse soft branch but leaves a longitudinal one. The stronger relative-phase constraint gives a uniform frequency floor in the same quadratic model.

8.2 Dependence on current inertia

The value in Theorem 8.1 assumes that the current is an independent oscillator with unit inertia. Keep $w = c = m_\theta = 1$, set $m_u \geq 0$, and retain the completion gap $\sqrt{2}$. For $m_u > 0$, the zero-momentum generalized characteristic equation and its lower root are

$$m_u\mu^2 - (1 + 2m_u)\mu + 1 = 0, \qquad \mu_-(m_u) = \frac{2}{1 + 2m_u + \sqrt{1 + 4m_u^2}}, \quad \Delta_{\text{lock}} = \sqrt{\mu_-(m_u)}.$$

Positive gradient additions leave this as the all-momentum lower edge. For $m_u = 0$, the inertia is singular and the current must be eliminated algebraically, rather than treated with an inverse kinetic matrix. At zero momentum $u = -\theta$, leaving stiffness one and gap exactly one. More generally the transverse stiffness is $1 + q$ and the longitudinal stiffness is $2 - (1 + q)^{-1}$; their infimum is one. The lower eigenvalue formula tends continuously to this result as $m_u \downarrow 0$, while the extra current oscillator moves to infinite frequency.

Current inertia m_u	**Hard-locked gap**
0 (algebraic)	1.000000
0.1	0.949200
0.5	0.765367
1	0.618034

This sensitivity is consistent with Section 9.5: an independent variational current in the local master-action restriction need not have its own time derivative. Giving it unit inertia is an explicitly chosen kinetic completion. The table does not select which completion the physical history dynamics returns.

8.3 Finite pinning connects the soft and locked models

Add the finite gauge-invariant contribution $\rho \parallel y - d\phi \parallel^2$ to $2S$. In the gauge $\phi = 0$, with $w = w_J$, the onsite quadratic form is $w(u + \theta)^2 + c(\theta - y)^2 + \rho y^2$. Its matrix is

$$A(w, c, \rho) = \begin{pmatrix} w + c & w & -c \\ w & w & 0 \\ -c & 0 & c + \rho \end{pmatrix}, \qquad \det A(w, c, \rho) = wc\rho.$$

Theorem 8.2 (soft-lock family). Assume $w, c, \rho \geq 0$, finite nonnegative gradient coefficients, a fixed positive definite kinetic matrix and a positively gapped completion coordinate. The parent has a positive volume-uniform normal-mode gap if and only if w, c, ρ are all strictly positive. For positive coefficients and $M \preccurlyeq M_{\max} I$, a squared-frequency lower bound is $\min\{\lambda_{\min}\big(A(w, c, \rho)\big), m_\eta^2\}/M_{\max}$. Here m_η^2 denotes the completion stiffness in the same coordinates.

Proof. For positive w, c, ρ, the leading principal minors are $w + c$, wc and $wc\rho$, so the onsite form is positive definite. The transverse and longitudinal gradient additions are $\text{diag}(aq, 0, bq)$ and $\text{diag}(0, w_T q, 0)$ and are nonnegative. The generalized Rayleigh quotient gives the bound. If any onsite coefficient vanishes, the sum-of-squares form has a nonzero null vector. Its gradient energy is $O(q)$ and its kinetic norm stays positive as $q \to 0$, so no volume-uniform positive gap remains. This converse uses

the declared unquotiented parent and fixed kinetic coefficients; deleting a physical redundancy would change its carrier.

For unit $w = c = 1$ and all three unit inertias, the exact squared gap is $\mu_\rho = \lambda_{\min}\big(A(1,1,\rho)\big)$, the smallest root of

$$p_\rho(\mu) = \mu^3 - (4+\rho)\mu^2 + (3+3\rho)\mu - \rho.$$

It increases strictly with ρ, has $\mu_\rho = \rho/3 + O\big(\rho^2\big)$ near zero and tends to $\mu_0 = \big(3-\sqrt{5}\big)/2$ as $\rho \to \infty$. Increasing pinning adds a positive rank-one form; the lowest eigenvector has nonzero record component. At zero pinning the normalized null vector is $(1,-1,1)/\sqrt{3}$, giving the slope $1/3$. At large pinning, bounded energy forces $y \to 0$; the variational principle gives the two hard-lock branches while the third diverges. Thus Theorem 7.1 is the $\rho = 0$ endpoint and Theorem 8.1 is the unit hard-lock limit.

Pinning ρ	**Squared gap μ_ρ**	**Frequency gap**
0.1	0.031529	0.177563
1	0.198062	0.445042
10	0.355197	0.595984
Hard-lock limit	0.381966	0.618034

Uniform positive lower bounds on the three onsite coefficients, an upper bound on positive inertia and a positive completion floor give a uniform family bound. Positivity separately at each regulator is weaker. Finite pinning retains a dynamical relative record phase; it does not assert exact record freezing.

The static elimination of y at zero momentum gives the effective mass coefficient $c_{\text{eff}} = c\rho/(c+\rho)$. With a live record the frequency-dependent subtraction also carries memory, so c_{eff} alone is not the quantum gap. In the unit three-inertia model the trial vector gives $\mu_\rho \le \rho/3$. Consequently a physically dimensioned pinning coefficient tending to zero under refinement closes this gap. The physical question is therefore what selects ρ and its scaling relative to the kinetic terms, not merely whether a formal hard lock can be written.

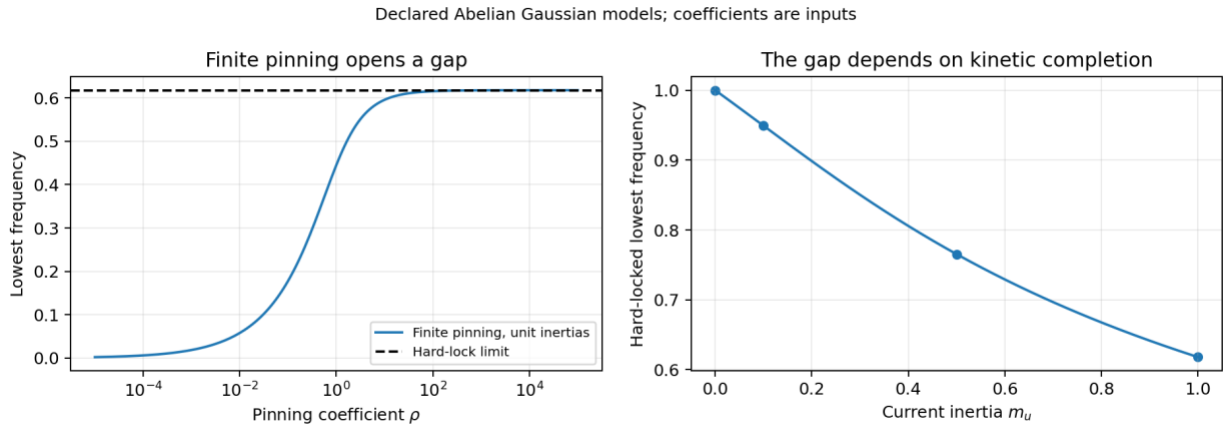


Figure 3. Finite pinning opens a gap in the declared Abelian Gaussian parent. The hard-lock value depends on current inertia. All coefficients are model inputs; neither panel predicts a physical Yang–Mills mass.

8.4 The algebraic-current theorem

The independent variational current in Section 9.5 need not carry a time derivative. Treat it algebraically, take $w_J > 0$ and $w_T \geq 0$, and give θ and y equal positive inertia m_{f}. This removes the optional current oscillator but still declares the field and record kinetics. Stationarity of the full spatial action gives

$$u = -\left(w_J I + w_T dd^{\dagger}\right)^{-1} w_J \theta.$$

Transversely $u = -\theta$; longitudinally $u = -w_J\theta/\left(w_J + w_T q\right)$. The current determinant from Gaussian integration is independent of θ, y for these fixed coefficients, so it does not alter their stiffness. On the two remaining coordinates define

$$B(c,\rho) = \begin{pmatrix} c & -c \\ -c & c+\rho \end{pmatrix}, \qquad K_T = B + \mathrm{diag}(aq, bq),$$

$$K_L = B + \mathrm{diag}\left(\frac{w_J w_T q}{w_J + w_T q}, 0\right).$$

Theorem 8.3 (native algebraic-current gap). For $c, \rho, m_{\mathrm{f}} > 0$ and nonnegative spatial coefficients, the phase-sector squared-frequency floor is

$$\Delta^2_{\mathrm{phase}} = \frac{\beta_-}{m_{\mathrm{f}}}, \qquad \beta_{\pm} = c + \frac{\rho}{2} \pm \frac{1}{2}\sqrt{4c^2 + \rho^2}.$$

The full gap is the smaller of this phase gap and the separately specified completion gap. If $a = b > 0$, both transverse polarizations have the exact continuum dispersions

$$\omega^2_{\pm}(k) = \frac{a}{m_{\mathrm{f}}}|k|^2 + \frac{\beta_{\pm}}{m_{\mathrm{f}}}.$$

In the hard-lock limit only θ remains, with transverse dispersion $\omega_T^2 = \left(a|k|^2 + c\right)/m_{\mathrm{f}}$ and phase gap $\sqrt{c/m_{\mathrm{f}}}$. On a spatial lattice replace $|k|^2$ by $q_\epsilon(k)$; exact relativistic dispersion here refers to the continuum branches, after fixing their common propagation speed.

Proof. Eliminate the algebraic current as above. The characteristic polynomial of B is $\beta^2 - (2c+\rho)\beta + c\rho$, giving $\beta_{\pm}$. Both momentum corrections are nonnegative, so the infimum is attained at $q = 0$ or approached by nonzero momenta at increasing volume. When $a = b$, the transverse correction is a multiple of the identity. Sending $\rho \to \infty$ suppresses y; the lower onsite eigenvalue tends to c and the upper one diverges. These statements prove the gap and branch formulas.

The weight w_J cancels from the transverse spectrum and the phase-gap floor, but not from the longitudinal dispersion. In the hard-lock limit the latter is $\omega_L^2 = [c + w_J w_T q/\left(w_J + w_T q\right)]/m_{\mathrm{f}}$. It saturates at large q when $w_T > 0$ and is not relativistic. Thus the result resolves the current-inertia ambiguity for this declared algebraic-current completion, and part of the transverse dispersion caveat, without establishing a relativistic theory on the complete carrier.

Pinning ρ	**Algebraic-current gap**	**Unit current-inertia gap**
0.01	0.070622	0.057575
0.1	0.220796	0.177563
1	0.618034	0.445042

Pinning ρ	Algebraic-current gap	Unit current-inertia gap
10	0.949200	0.595984
Hard-lock limit	1.000000	0.618034

The table uses $c = m_f = 1$ and a completion gap above the phase floor. Small pinning gives $\Delta^2_{\text{phase}} = \rho/(2m_f) + O\left(\rho^2/(cm_f)\right)$. The repeated value near 0.618 at finite native pinning and in the different unit-current hard-lock model is an equality of two particular quadratic eigenvalues, not a universal constant.

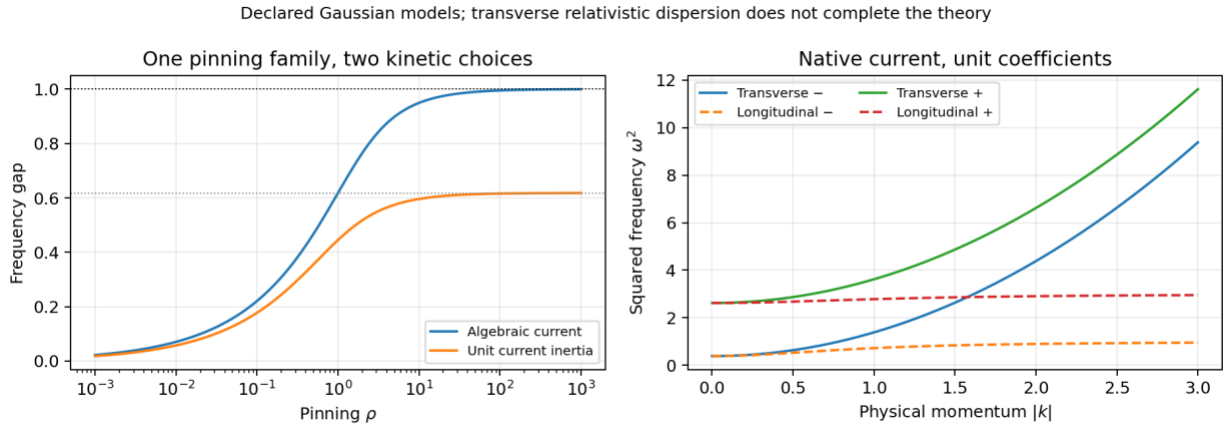


Figure 4. Algebraic elimination changes the pinning curve and hard-lock limit. With equal transverse gradient coefficients the native transverse squared frequencies are affine in momentum squared. The longitudinal branches remain nonrelativistic. All coefficients are inputs.

8.5 Relation to rigorous Higgs-phase results

Theorem 8.1 belongs beside established Higgs-mechanism gap results. Balaban, Imbrie, Jaffe and Brydges prove exponential clustering for gauge-invariant observables in a weakly coupled Abelian Higgs theory on a unit lattice, with strictly positive reference masses and sufficiently small interactions [25, Theorem 4.1]. This is an interacting relative of the Gaussian mass mechanism. It is not a theorem for the present auxiliary-current action, and it does not itself remove the lattice regulator.

Osterwalder and Seiler establish a rigorous Higgs regime by a lattice cluster expansion [26]. As Seiler explains [28, §1], a Yang–Mills–Higgs model with complete symmetry breakdown can have a gap even at arbitrarily weak gauge coupling when the Higgs potential is sufficiently strong. The regime and symmetry-breaking hypotheses matter: weak gauge coupling by itself is not a mass-gap theorem for pure Yang–Mills.

Fradkin and Shenker treat fixed-length Higgs fields and establish an analytic connection between confinement and Higgs regions in the applicable fundamental-representation setting [27]. In a suitable unitary gauge the Higgs orientation can be fixed; its gauge coupling remains in the action. This motivates the frozen-phase analogy, rather than proving that the additional field was absent. Their analyticity result is not a continuum pure Yang–Mills existence theorem.

The specific VERSF proposal is that commitment supplies the fixed reference or its finite stiffness ρ, rather than importing an independent physical Higgs sector. Establishing that proposal requires a map from the actual committed carrier and common dynamics to the reduced action, including the gauge quotient and reference motion. The cited Higgs results neither supply that map nor convert a gauge-plus-

matter model into pure Yang–Mills. A fixed Higgs modulus, a gauge-fixed orientation and an operationally frozen record are distinct assertions whose equivalence cannot be presumed.

9 Restoring strength, inertia and the common dynamics

9.1 The declared Gaussian transfer

To attach an energy to the quadratic stiffness, use the symmetric transfer form in Source History Weighting [6, §19.7, Eq. (164)], applied here to the specified bosonic parent. Let D be a constant positive diffusion matrix and define

$$L_D = -\frac{1}{2}\nabla \cdot D\nabla, \quad V(z) = \frac{1}{2}z^T K z, \quad T_{\delta t} = e^{-\delta t V/2} e^{-\delta t L_D} e^{-\delta t V/2}.$$

For the unit benchmark $D = I$. More generally, the squared frequencies are eigenvalues of $D^{1/2}KD^{1/2}$, equivalently the generalised stiffness eigenvalues for inertia $M = D^{-1}$. A stiffness coefficient without this normalisation is not an energy.

Proposition 9.1. For one positive quadratic eigenvalue μ, the exact excitation spacing of the normalised Gaussian transfer is

$$\Delta_{\delta t}(\mu) = \frac{2}{\delta t}\operatorname{arsinh}\left(\frac{\delta t\sqrt{\mu}}{2}\right).$$

Proof. The one-coordinate integral kernel is proportional to $\exp[-(x-y)^2/(2\delta t) - \delta t\mu(x^2+y^2)/4]$. Gaussian integration gives a ground state with precision $R_{\delta t} = \sqrt{\mu + \delta t^2\mu^2/4}$. Successive Hermite eigenvalues have ratio $r = \left(1 + \delta t R_{\delta t} + \delta t^2\mu/2\right)^{-1}$. Taking $-\log r/\delta t$ yields the displayed expression. Orthogonal diagonalisation gives the multi-coordinate result. Independent integral-kernel quadrature checks this formula.

For each fixed positive time step, the spacing tends to zero when μ tends to zero; as the time step vanishes it tends to $\sqrt{\mu}$. Thus the soft modes of Theorem 7.1 remain soft in an actual transfer spectrum. Under Theorem 8.1, the time-step-one gap has the uniform lower bound 0.608597929. This is the transfer of the declared Gaussian restriction, not a derived complete physical history Hamiltonian.

9.2 Derive both coefficients from one coupled kernel

Partition the coordinates on a fixed supported physical quotient into a retained coordinate x and all responding coordinates z. On a real reversible quadratic branch with constant symmetric kinetic matrix M, write $Q(\omega) = K + \omega^2 M$ and $K = \begin{pmatrix} A & B \\ B^T & K_{zz} \end{pmatrix}$, with K_{zz} positive on the eliminated support. Gaussian elimination gives

$$\Gamma_x(\omega) = Q_{xx} - Q_{xz}Q_{zz}^{-1}Q_{zx}.$$

Proposition 9.2. The zero-frequency restoring matrix and the coefficient of ω^2 in this same response are

$$K_x = A - BK_{zz}^{-1}B^T, \qquad M_x = \mathcal{E}^T M \mathcal{E}, \qquad \mathcal{E} = \begin{pmatrix} I \\ -K_{zz}^{-1}B^T \end{pmatrix}.$$

Proof. The zero-frequency minimiser is $z = -K_{zz}^{-1}B^T x$. Differentiating the exact Schur complement with respect to ω^2 at zero gives the pullback of M along that static relaxed lift. In components it retains both mixed kinetic blocks:

$$M_x = M_{xx} - M_{xz}K_{zz}^{-1}B^T - BK_{zz}^{-1}M_{zx} + BK_{zz}^{-1}M_{zz}K_{zz}^{-1}B^T.$$

This derives the induced inertia, not the primitive entries of M. For one retained scalar, K_x/M_x is a low-frequency estimate of squared frequency only when the expansion remains valid at that frequency. The full generalized spectrum of (K, M), or the poles of the complete response, supplies the actual oscillator frequencies. Scaling both forms by the same positive constant leaves their ratio and frequencies unchanged. Relative coefficients, the physical clock and their refinement behavior still matter. The common-response suite verifies the formula for noncommuting mixed matrices and under coordinate shears.

9.3 The same quantum spectrum supplies both responses

The analogous response identity applies beyond a harmonic bath. In a fixed physical source coordinate f, let the admitted Hamiltonian be $H(f) = H_0 + fV + f^2W_2/2$ to second order. Let $|0\rangle$ be a nondegenerate ground state, $\delta_n = E_n - E_0 > 0$, and retain any primitive kinetic term $m_0\dot{f}^2/2$ derived from the same parent. The connected zero-temperature response is

$$\Gamma_f(i\omega) = m_0\omega^2 + \langle W_2\rangle - 2\sum_{n>0}\frac{\delta_n|V_{n0}|^2}{\delta_n^2 + \hbar^2\omega^2}.$$

$$K_f = \langle W_2\rangle - 2\sum_{n>0}\frac{|V_{n0}|^2}{\delta_n}, \qquad M_f = m_0 + 2\hbar^2\sum_{n>0}\frac{|V_{n0}|^2}{\delta_n^3}.$$

The same excitation energies and couplings reduce static curvature and add delayed inertia. Expanding the spectral denominator proves the pair when the sums and low-frequency expansion converge. A gapless unresolved bath may produce divergent coefficients or nonanalytic response, requiring the unexpanded kernel. In the continuum the sums become spectral integrals. The physical-response paper already identifies this delayed response and the required velocity connection when a source is relocated by a parameter-dependent unitary transformation [12, §§16.12–16.13]. That connection, and any multi-source Berry term, must be retained. An externally imposed probe response alone is not a propagating particle mass.

For a harmonic bath with stiffness K_b, inertia M_b and coupling fb^Tz, these sums reduce to $K_f = \langle W_2\rangle - b^TK_b^{-1}b$ and $M_f = m_0 + b^TK_b^{-1}M_bK_b^{-1}b$. Thirty noncommuting examples recover the complete Schur response independently. This checks the common spectral derivation; it does not evaluate the unknown interacting Yang–Mills spectrum.

9.4 The restoring strength and inertia of the surviving mode

For the longitudinal restriction of Section 7, write $w = w_J$, $t = w_T$ and retain $c > 0$. The static potential is $2S_L = w(u+\theta)^2 + tqu^2 + c(\theta - y)^2$. On this same chart supply a diagonal kinetic completion with entries (m_θ, m_u, m_y). These entries remain explicit inputs, rather than claimed physical selections. Eliminate both current and record response:

$$\Gamma_\theta(\omega) = w + c + m_\theta\omega^2 - \frac{w^2}{w + tq + m_u\omega^2} - \frac{c^2}{c + m_y\omega^2}.$$

$$K_\theta = \frac{wtq}{w+tq}, \qquad M_\theta = m_\theta + m_y + \frac{w^2 m_u}{(w+tq)^2}.$$

The static response of the current is $-w/(w+tq)$ and that of the record is 1. Their kinetic costs enter with the squares of those response factors. A general mixed kinetic matrix uses Proposition 9.2 with $\mathcal{E} = (1, -w/(w+tq), 1)^T$. In the declared unit completion,

$$K_\theta = \frac{q}{1+q}, \qquad M_\theta = 2 + \frac{1}{(1+q)^2} \to 3, \qquad \omega_{\min} \sim \sqrt{q/3}.$$

The restoring strength vanishes while inertia stays finite. The complete three-coordinate eigenproblem verifies the asymptotic frequency, so it is not inferred solely from a derivative expansion. With algebraic current instead, $m_u = 0$ and unit field and record inertias give $M_\theta = 2$ and $\omega_{\min} \sim \sqrt{q/2}$; that admissible diagnostic completion also remains soft.

The locked model has the same kinetic ambiguity: eliminating an algebraic current gives gap one for the unit field coefficient, whereas retaining unit current inertia gives approximately 0.618. Section 8.2 derives the entire interpolation. Changing the current inertia thus changes both the unpinned soft response and the positive pinned spectrum; neither choice is selected by the static action alone.

Sites per direction N	Restoring strength	Induced inertia	Exact unit-parent frequency
32	0.037007271	2.927354997	0.111977403
128	0.002403298	2.995199180	0.028318811
512	0.000150574	2.999698875	0.007084813

Here $q = 4\sin^2(\pi/N)$ and spatial spacing is one. All frequencies use the declared reference clock and primitive kinetic completion. They are not physical glueball masses.

Proposition 9.3. In the unchanged longitudinal spatial parent, for any positive mixed inertia $M(q)$ and admitted trial direction $v = (1, -1, 1)^T$,

$$\omega^2_{\min}(q) \le \frac{v^T K_L(q) v}{v^T M(q) v} = \frac{tq}{v^T M(q) v}.$$

Proof. This is the generalized Rayleigh variational bound; the two mismatch terms vanish on v. If its kinetic norm stays bounded away from zero as $q \to 0$, the nonnegative lowest squared frequency tends to zero. Thus regular mixed inertia alone cannot repair this parent. The physical dynamics must exclude the direction, change its restoring behavior, or establish different kinetic behavior with a valid measure and refinement limit. Consistently reparametrizing a longitudinal coordinate multiplies both forms and cannot remove the soft spectrum.

9.5 Continuity induces density inertia without a current oscillator

The independent variational current of the local master-action restriction need not carry an independent time derivative [13]; Appendix B.1 derives its auxiliary reconstruction. The literal constitutive and continuity defects contain a density response. On one positive scalar Laplacian mode, let r denote density amplitude, j longitudinal current, κ the constitutive coefficient, and v_r a supplied density-potential curvature:

$$2\mathcal{A} = \int [w_J\big(j - \kappa\sqrt{q}\, r\big)^2 + w_T\big(\dot{r} + \sqrt{q}\, j\big)^2 + v_r r^2]dt.$$

Eliminating the algebraic j, including its response to $\dot{r}$, gives the following exact bulk coefficients, up to the retained endpoint boundary term:

$$M_r = \frac{w_J w_T}{w_J + w_T q}, \qquad K_r = v_r + \kappa^2 q^2 M_r, \qquad \omega_r^2 = \kappa^2 q^2 + \frac{v_r}{M_r}.$$

For $v_r = 0$, $\omega_r = |\kappa| q$ still tends to zero. A positive density curvature is not automatically a restoring term for the distinct gauge-fixed phase of Section 9.4. These are Euclidean history rates; physical quantum interpretation additionally needs the admitted transfer and clock. This calculation does not add a second current noise or a primitive current mass.

Mixed first derivatives are essential. For a defect history $\big(J\zeta + T\dot{\zeta}\big)^T W\big(J\zeta + T\dot{\zeta}\big)/2$ plus static curvature V, set $K = J^T W J + V$, $M = T^T W T$ and $G = J^T W T - T^T W J$. The kernel is $K + i\omega G + \omega^2 M$. Use the static lift $\mathcal{E}$ of Proposition 9.2 and let Z insert the eliminated coordinates, with $G_{xz}^{'} = \mathcal{E}^T G Z$. Expansion of its Schur complement yields

$$G_x = \mathcal{E}^T G \mathcal{E}, \qquad M_x = \mathcal{E}^T M \mathcal{E} - G_{xz}^{'} K_{zz}^{-1} \big(G_{xz}^{'}\big)^T.$$

The subtractive term is required; omitting it would incorrectly give $M_r = w_T$ above. Any surviving G_x must also be retained. Configuration Dynamics already derives continuity-induced inertia on its finite quotient and explains that the operational kinetic sector was omitted from that restriction [14, IV.17]. Frequency independence of its particular transverse response therefore does not mean that physical gauge fields have zero dynamics.

9.6 Internal current inertia and the limits of a stiffness ratio

Consider the explicit four-coordinate internal Gaussian precursor on (p, q, θ, y). Its stiffness and optional kinetic matrix are

$$K_4 = \begin{pmatrix} 1 & 0 & -1/\sqrt{2} & 0 \\ 0 & 1 & 1/\sqrt{2} & 0 \\ -1/\sqrt{2} & 1/\sqrt{2} & 6 & -1 \\ 0 & 0 & -1 & 5 \end{pmatrix}, \qquad M_4 = \mathrm{diag}(0,0,m,m).$$

The phase inertia m is an explicitly optional source parameter. Eliminating both currents leaves the phase stiffness $\begin{pmatrix} 5 & -1 \\ -1 & 5 \end{pmatrix}$ and exact frequencies $2/\sqrt{m}$ and $\sqrt{6/m}$. Alternatively, retain current p and eliminate the other three coordinates. With $z = m\omega^2$, the exact response and its low-frequency coefficients are

$$\Gamma_p(\omega) = \frac{z^2 + 10z + 24}{z^2 + (21/2)z + 53/2}, \qquad K_p = \frac{48}{53}, \qquad M_p = \frac{52m}{2809}.$$

Current inertia is induced entirely through the moving phase pair. No additional primitive current oscillator has been introduced. For $m = 1$, the estimate $\sqrt{K_p/M_p} = 6.994503$ lies beyond the low-frequency expansion regime, whereas the actual phase poles are 2 and $\sqrt{6} = 2.449490$. Both poles occur in the current covariance, which also has an inherited contact term. This explicit discrepancy is why a positive local restoring coefficient and induced inertia do not by themselves determine an excitation threshold when response has memory. The finite internal precursor is not a continuum Yang–Mills gap.

9.7 Reconstruct both forms from one history law

Suppose the complete joint history returns a stationary reversible Gaussian transition $q_{n+1} = Fq_n + \xi_n$ with innovation covariance Q_ξ, physical step τ, nonsingular supported stationary covariance, and eigenvalues of F strictly between zero and one. All cross correlations must be included. Fourier transformation of the innovation action gives a lattice precision $K_{\mathrm{lat}} + \hat{\omega}^2 M_{\mathrm{lat}}$, where $\hat{\omega} = 2\sin(\omega\tau/2)/\tau$, with

$$M_{\mathrm{lat}} = \tau Q_\xi^{-1} F, \qquad K_{\mathrm{lat}} = \tau^{-1}(I - F)^T Q_\xi^{-1}(I - F).$$

Reversibility makes $Q_\xi^{-1}F$ symmetric positive. Both coefficients are returned by the same conditional mean and innovation covariance. For the Gaussian heat sandwich they recover the supplied action pair. This is a consistency check, not physical selection of the supplied kinetic operator.

The finite-step Hamiltonian is instead $-\log T/\tau$. Solve $\Sigma = F\Sigma F^T + Q_\xi$ and set $A_\tau = -\log F/\tau$. On this reversible Gaussian branch its exact differential oscillator representation, up to vacuum energy and with $\hbar = 1$, has

$$D_\tau = 2A_\tau\Sigma, \qquad M_\tau = D_\tau^{-1}, \qquad K_\tau = A_\tau^T M_\tau A_\tau.$$

Detailed balance makes D_τ symmetric positive. The oscillator frequencies are the eigenvalues of A_τ, recovering Proposition 9.1 for a heat sandwich. Thirty-six noncommuting positive matrix examples reconstruct both the action pair and the logarithmic Hamiltonian pair. A reduced process with memory cannot be silently replaced by a one-step Markov law. The physical source must supply this full joint transition, or the corresponding complete generator and measure on its actual branch; a record-label transition and one scalar event rate are insufficient.

9.8 What these derivations physically select

The common-kernel identities determine how restoring strength and inertia follow from complete dynamics. The currently returned physical construction still has to supply that complete dynamics on the admitted current–matter–record carrier [12,15]. In particular, HMGBC distinguishes operational geometry, which fixes kinetic motion and volume, from the defect weighting returned to the master action [15, §4 and §56A]. Appendix B.2 derives why joint kinetic reduction must preserve mixed blocks and the induced measure. Setting the kinetic metric equal to static defect stiffness would be an additional physical identification.

The parameter-closure analysis already identifies the identity response obtained by inverting the same defect map as an algebraic consequence [16, §71.2]. The present control verifies this directly: for the three-mode defect matrix with rows $(1,1,0)$, $(1,0,-1)$ and $\left(0,\sqrt{q},0\right)$, choosing $W = (JJ^T)^{-1}$ forces $J^T W J = I$ but requires a divergence-sector weight $W_{33} = 3/q$. That singular choice is not the original finite-weight parent. These distinctions avoid fitting inertia or weighting to a desired gap and keep previously integrated fluctuations counted once.

10 Infinite volume and removal of the regulators

10.1 A specified family in physical units

We now state the refinement prescription explicitly. Let $\epsilon > 0$ be spatial spacing, $R = N\epsilon$ the periodic physical side, and $\delta t > 0$ the time step. Keep the full relative-phase constraint, the physical gradient coefficients, $w = c = 1$, completion stiffness two and identity inertia fixed. Set $\hbar = 1$ and choose fixed reference length and time units. This is a declared continuum family; it is not an established VERSF renormalization trajectory.

$$d_{\epsilon,i}(k) = \frac{2}{\epsilon}\sin\left(\frac{\epsilon k_i}{2}\right), \qquad k_i = \frac{2\pi n_i}{R}, \qquad q_\epsilon(k) = |d_\epsilon(k)|^2.$$

The full reduced stiffness on (θ, u, η) has seven components and takes the form below. The same form with $d = k$ defines its continuum symbol.

$$K(d) = \begin{pmatrix} (|d|^2 + 2)I - dd^T & I & 0 \\ I & I + dd^T & 0 \\ 0 & 0 & 2 \end{pmatrix}.$$

Both kinetic and potential real-space forms carry the cell volume ϵ^3. The canonical change $z = \epsilon^{3/2} f$ removes that common factor, leaving the displayed frequency matrix. Thus adding sites does not insert a spurious power of the volume into the energy. Theorem 8.1 applies with $q = q_\epsilon(k)$ and gives $K_{\epsilon,R} \succcurlyeq \mu_0 I$ at every momentum, size and spacing.

10.2 Conditional Gaussian continuum theorem

Theorem 10.1. For the family specified in Section 10.1, the infinite-volume continuum free-field Hamiltonian exists in its Gaussian Fock representation and has gap exactly $\sqrt{\mu_0}$. Its finite-regulator Gaussian transfers obey a positive uniform energy bound for $0 < \delta t \le 1$, and their smeared covariance limit agrees with that continuum theory as $\epsilon \to 0$, $R \to \infty$ and $\delta t \to 0$.

Proof, spatial operator. On $\mathcal{H}_1 = L^2(\mathbb{R}^3; \mathbb{C}^7)$, with the usual reality structure for the seven real fields, define the self-adjoint Fourier multiplication operator $K(k)$ from Section 10.1 on its maximal domain. Equivalently, it is associated with the closed positive form

$$\mathfrak{q}[\theta, u, \eta] = \int_{\mathbb{R}^3} \left(|\mathrm{curl}\theta|^2 + |\nabla \cdot u|^2 + |u + \theta|^2 + |\theta|^2 + 2|\eta|^2\right) d^3x.$$

The onsite bound gives $K \succcurlyeq \mu_0 I$. At each fixed physical momentum, $d_\epsilon(k) \to k$, and the symbols converge with order-ϵ^2 error on bounded momentum sets. To compare finite boxes, embed discrete Fourier vectors as normalised constant functions on momentum cells of width $2\pi/R$, within the lattice Brillouin zone. The resulting averaging projections tend strongly to the identity when $R \to \infty$ and $\epsilon \to 0$. On any fixed compact momentum set the matrix symbols converge, while $\left(K_{\epsilon,R} + I\right)^{-1}$ is uniformly bounded by $(1 + \mu_0)^{-1}$. Approximation by compactly supported momentum functions and dominated convergence therefore give strong convergence of the embedded resolvents. No operator-norm convergence across all ultraviolet modes is asserted.

Proof, vacuum and excitations. Set $\mathcal{W} = \sqrt{K}$ and define $H = d\Gamma(\mathcal{W})$ on bosonic Fock space, normal ordered relative to its vacuum. On the n-particle sector, $H \succcurlyeq n\sqrt{\mu_0}$. The vacuum is the unique zero-

energy vector. Normalised one-particle wave packets supported near $k = 0$ approach the lowest eigenfrequency, so the spectral gap is exactly, rather than only at least, $\sqrt{\mu_0}$.

$$H \geqslant \sqrt{\mu_0}(I - P_{\mathrm{vac}}), \qquad \mathrm{gap}(H) = \sqrt{\mu_0} = 0.618033989\ldots.$$

The free Euclidean vacuum covariance is $G_E(t,k) = 1/2\,K(k)^{-1/2}e^{-|t|\sqrt{K(k)}}$. Spatially smeared correlations are well-defined. This explicitly specifies the limiting vacuum instead of dividing an infinite product of finite-volume transfer eigenvalues. Normal ordering subtracts an additive vacuum energy and does not change excitation spacings.

Proof, time regulator. Proposition 9.1 defines an increasing function of $\sqrt{\mu}$. Therefore the regulated gap is at least $2\mathrm{arsinh}\left(\delta t\sqrt{\mu_0}/2\right)/\delta t$, which is at least 0.608597929 for $\delta t \leq 1$ and approaches $\sqrt{\mu_0}$ as the time step vanishes. At each fixed momentum the transfer eigenfrequencies and Gaussian precisions converge to the continuum ones. The position covariance is uniformly bounded by $1/\left(2\sqrt{\mu_0}\right)$; smooth test functions control the remaining high-momentum factors. These bounds and the Fourier embeddings give the joint smeared-correlation limit. The argument does not assume a uniform Trotter error for unbounded frequencies. This completes the construction for the stated Gaussian family.

Corollary 10.2 (fixed finite pinning). Keep a fixed physical $\rho > 0$ and all unit coefficients and inertias of Theorem 8.2. On the ten-component real-field carrier, the form is the sum of $|\mathrm{curl}\theta|^2$, $|\mathrm{curl}y|^2$, $|\nabla \cdot u|^2$, $|u+\theta|^2$, $|\theta - y|^2$, $\rho|y|^2$ and $2|\eta|^2$. The same multiplication-operator and Fock construction gives a continuum gap exactly $\sqrt{\mu_\rho}$. The positive bound and the fixed-momentum convergence arguments of Theorem 10.1 apply with μ_0 replaced by μ_ρ. This extends the conditional continuum result to finite pinning; it does not derive the coefficient or justify a trajectory on which it collapses.

Corollary 10.3 (native-current continuum). For the constant positive physical coefficients and equal field inertias of Theorem 8.3, the seven real coordinates (θ, y, η) define a Gaussian continuum theory after algebraic current elimination. Its gap is $\min\{\sqrt{\beta_-/m_{\mathrm{f}}}, \Delta_\eta\}$. The hard-locked four-coordinate theory has gap $\min\{\sqrt{c/m_{\mathrm{f}}}, \Delta_\eta\}$. These equalities assume the corresponding completion gap $\Delta_\eta > 0$.

Proof. Assemble the transverse and longitudinal blocks in Theorem 8.3 into their spatial Fourier multiplier. The rational longitudinal correction is nonnegative and continuous at $k = 0$, since $w_J > 0$. The onsite bound, convergence of d_ϵ on bounded momenta and bounded resolvents give the same strong-resolvent and smeared-covariance argument as Theorem 10.1. Second quantization gives the unique Fock vacuum and stated gap. Low-momentum wave packets approach the phase floor; the completion supplies its own floor. Eliminating the auxiliary current can make the spatial response nonlocal, so this construction is not a claim of relativistic locality.

10.3 Executed volume and regulator tests

The joint limit was evaluated with $\delta t = \epsilon$ while increasing the physical side. The values below use the lowest nonzero momentum. Including the constant mode gives the same normal-mode lower bound exactly at every finite volume; excluding it does not change the continuum infimum.

Physical side R	Spacing and time step	Lowest nonzero-mode energy
8	1	0.704176
32	0.25	0.625850

Physical side R	Spacing and time step	Lowest nonzero-mode energy
128	0.0625	0.618534
512	0.015625	0.618065
1024	0.0078125	0.618042

At fixed physical side $R = 16$, refinement approaches the nonzero-mode continuum frequency 0.650021322; the subsequent volume limit approaches 0.618033989. The full symbols and resolvents show the expected second-order convergence on the tested fixed wavevectors. For a Gaussian spatial test with $|\hat{f}(k)|^2 = e^{-|k|^2}$, the trace of the seven smeared equal-time covariances approaches 0.06618576526, independently confirmed by a radial continuum integral.

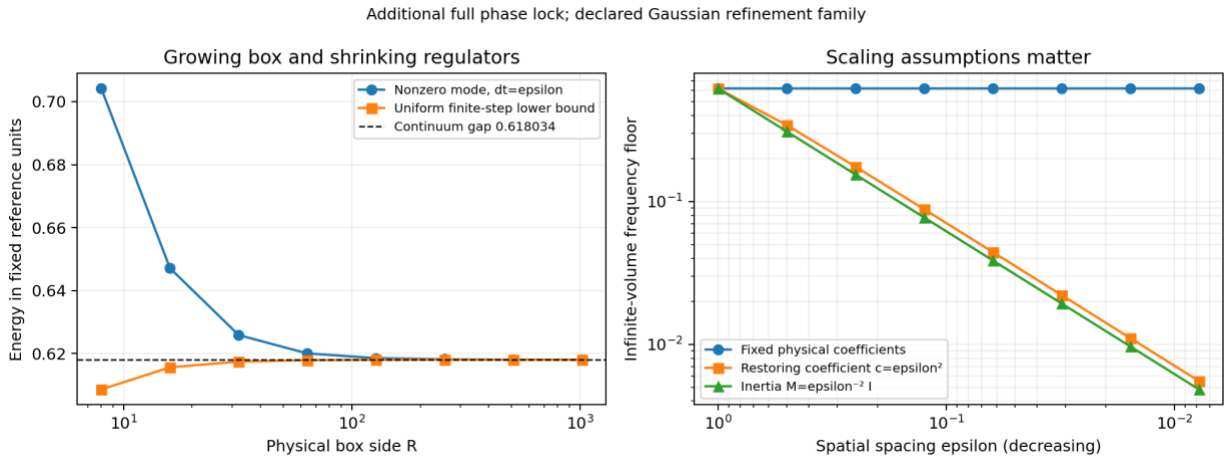


Figure 5. The positive bound survives the declared joint volume and regulator limit. Alternative positive-at-each-spacing coefficient families can nevertheless close the gap. All energies use fixed reference units, with the full relative-phase constraint imposed.

Scope. Theorem 10.1 has Gaussian auxiliary branches with frequencies bounded at large momentum, so it is not a relativistic pure Yang–Mills construction. The native-current version gives the relativistic transverse branches of Theorem 8.3 but retains a nonrelativistic longitudinal sector. The next subsection states which axiomatic properties do hold. None of these theorems proves that the full VERSF dynamics selects the reduced variables, coefficients or vacuum representation.

10.4 Axiom scorecard and temporal positivity

The Jaffe–Witten problem asks for a nontrivial quantum Yang–Mills theory on $\mathbb{R}^4$ for every compact simple gauge group, with a positive mass gap and axiomatic properties at least as strong as the cited Wightman or Osterwalder–Schrader framework [1]. Theorem 10.1 constructs a smaller Gaussian theory. The following properties can be established directly, without assuming full Euclidean invariance.

Proposition 10.4 (time reflection positivity and clustering). For the Gaussian Fock construction with $\mathcal{W} \geq \Delta I > 0$, its covariance $G_E(t) = 1/2\, \mathcal{W}^{-1} e^{-|t|\mathcal{W}}$ is reflection positive across $t = 0$. For a spatially smeared test function $f(t)$ supported at positive times,

$$\int_0^\infty \int_0^\infty \langle f(t), G_E(t+s) f(s) \rangle \, dt \, ds = \frac{1}{2} \| \mathcal{W}^{-1/2} \int_0^\infty e^{-t\mathcal{W}} f(t) \, dt \|^2 \geq 0.$$

Proof. Factor the positive semigroup using self-adjoint spectral calculus, giving the displayed norm square. Positivity of this reflected covariance gives reflection positivity of the centered Gaussian measure. For bounded observables A, B, or smeared operators with the required finite vacuum-vector norms, the vacuum spectral gap also gives

$$|\langle 0|Ae^{-tH}B|0\rangle - \langle A\rangle\langle B\rangle| \leq e^{-\Delta t} \| P_\perp A^\dagger |0\rangle \| \, \| P_\perp B|0\rangle \|.$$

Here $P_\perp = I - P_{\text{vac}}$. Insert $P_\perp$ on both sides of the semigroup and use $\| e^{-tH} P_\perp \| \leq e^{-\Delta t}$. For Theorem 10.1, $\Delta = \sqrt{\mu_0}$. The finite-pinning and native-current constructions use their own gaps. This is temporal exponential clustering; it does not assert isotropic spacetime clustering at that rate.

Property	**Status for Theorem 10.1**
Continuum Gaussian field and tempered covariance	Established by the multiplier and smeared-covariance construction.
Reflection positivity across time zero	Established by Proposition 10.4; this alone is not the full OS axiom system.
Unique vacuum and positive energy gap	Established in the declared Fock representation; gap $\sqrt{\mu_0}$.
Exponential clustering in Euclidean time	Established with rate $\sqrt{\mu_0}$ for the stated observables.
Translations and spatial rotations	Present for the continuum symbol, with vector and scalar fields transformed accordingly.
Full four-dimensional Euclidean invariance	Fails for the declared complete field theory: the auxiliary branches do not share relativistic dispersion. Full relativistic reconstruction is not established.
Compact simple non-Abelian gauge theory	Absent. The construction is an Abelian phase restriction with auxiliary coordinates.
Interacting Yang–Mills nontriviality	Absent. The theory is Gaussian, with no connected linear-field correlations above order two.

The Gaussian theory is not the zero theory: its two-point function and excitations are nonzero. What is absent is interacting Yang–Mills dynamics. The lack of full Euclidean invariance is explicit even in the completion scalar, whose covariance in spacetime momentum is $\left(p_0^2 + 2\right)^{-1}$, independent of spatial momentum. A Euclidean rotation mixing time and space changes it. The native-current transverse branches repair one dispersion issue, while their longitudinal and completion sectors still do not supply a fully relativistic non-Abelian theory.

11 Scaling and interaction conditions that remain essential

11.1 Physical normalisation and collapsing positive coefficients

For the path $\delta t = \epsilon$, rewriting the same fixed-physical-coefficient family in lattice units gives $K_{\mathrm{lat}} = \epsilon^2 K_{\mathrm{phys}}$. Its dimensionless onsite coefficients scale as ϵ^2 and its physical transfer energy is the lattice energy divided by ϵ. This conversion was checked against the direct physical calculation. Keeping the old dimensionless unit matrices fixed while shrinking the time unit instead produces a physical gap proportional to $1/\epsilon$; it does not demonstrate a finite continuum mass scale.

Even with the full hard constraint intact, choosing $w = 1$ and $c(\epsilon) = \epsilon^2$ yields $\alpha(1, c) \sim \epsilon^2/2$ and a gap tending to zero as $\epsilon/\sqrt{2}$. Here the restoring coefficient changes; the constraint itself is not softened. With fixed stiffness and inertia $M(\epsilon) = \epsilon^{-2} I$, the gap instead equals $\epsilon\sqrt{\mu_0}$. Positivity at each spacing is therefore weaker than the required uniform positive restoring strength relative to inertia.

In physical units the input Stueckelberg spatial mass ratio is c/a, and the energy scale additionally uses the kinetic normalization. Holding that ratio and the chosen inertias fixed preserves an assumed scale; it is not dynamical generation of a scale. For finite pinning with the other physical coefficients fixed, $\rho(\epsilon) = \epsilon^2$ gives $\Delta \sim \epsilon/\sqrt{3}$. A fixed dimensionless lattice pinning is a different prescription and requires the same conversion to physical units as every other onsite term.

For the algebraic-current model, the remaining phase-gap calculation is closed once the physical coefficients are known:

$$\Delta^2_{\mathrm{phase}}(c, \rho, m_{\mathrm{f}}) = \frac{2c\rho}{m_{\mathrm{f}}\left(2c + \rho + \sqrt{4c^2 + \rho^2}\right)}.$$

Two coefficient questions remain. First, which returned corpus quantities fix c, ρ and the field inertia in one physical coordinate and clock? The mismatch coefficient in the spatial action [6, Eq. (154)] provides the formal slot for c. The complete committed-record pullback and its jointly relaxed response must supply ρ or exclude the direction outright. The operational kinetic metric and history clock [14,15] must supply m_{f}. The cycle result of Section 5.3 alone does not determine these spatial physical coefficients. If the returned operators are anisotropic or have memory, a scalar two-coefficient reduction must itself be justified.

Second, does the physical refinement trajectory keep the normalized coefficients positive and finite? In this Gaussian family, after kinetic normalization and with $\delta t = \epsilon$ in calibrated units, define the dimensionless lattice onsite coefficients by

$$c^{\mathrm{can}}_{\mathrm{lat}} = \epsilon^2 \frac{c_{\mathrm{phys}}}{m_{\mathrm{f}}}, \qquad \rho^{\mathrm{can}}_{\mathrm{lat}} = \epsilon^2 \frac{\rho_{\mathrm{phys}}}{m_{\mathrm{f}}}, \qquad \Delta_{\mathrm{phys}} = \frac{\Delta_{\mathrm{lat}}}{\epsilon}.$$

Fixed positive physical ratios therefore require these normalized lattice coefficients to scale as ϵ^2, giving a finite positive physical phase gap. This is distinct from making the physically dimensioned ρ_{phys} vanish as ϵ^2, which closes the native gap as $\epsilon/\sqrt{2m_{\mathrm{f}}}$ for unit fixed c. For an interacting theory, renormalization and running can modify relations between bare parameters and these physical response coefficients; an unqualified bare-ϵ^2 law has not been proved. Answering these two questions would select the mass scale for this admitted Gaussian carrier. Physical admission, the remaining sectors and the interacting Yang–Mills identification remain additional tasks.

11.2 Positive interactions and the changing vacuum

The Gaussian theorem cannot be extended to an arbitrary nonlinear theory by observing that an added potential is nonnegative. Even in finite dimension, a positive perturbation can reduce the gap measured from the new vacuum energy. Take

$$H_0 = \mathrm{diag}(0,1,2), \qquad V_\delta = \mathrm{diag}(1-\delta, 0, 0), \qquad 0 < \delta < 1.$$

Then $V_\delta \geqslant 0$, but $H_0 + V_\delta$ has ground energy $1-\delta$ and gap δ. The relevant comparison must control the vacuum shift as well as the excitation form.

One sufficient, deliberately strong stability condition is available. If a self-adjoint perturbation preserves the old vacuum with $V|0\rangle = 0$, and on the vacuum-orthogonal form domain $V \geqslant -\eta H_0$ with a uniform $0 \leq \eta < 1$, then

$$H_0 + V \geqslant (1-\eta)\Delta_0(I - P_{\mathrm{vac}}).$$

The proof is direct addition of the two form inequalities, with the common vacuum fixed. A VERSF application would have to verify such a condition or provide another nonperturbative argument. Adding interactions can change the vacuum, create extra low-energy sectors or alter the kinetic measure; the quadratic calculation does not control those effects.

11.3 Relation to the strong-sector papers

The triality completion paper distinguishes an inserted centre-penalty reference Hamiltonian from a physically derived colour Hamiltonian, and makes continuum passage conditional on compatible refinement and form or transfer convergence [8, §§3.8, 20]. GQSC-1R exhibits compatible centre transfers with undetermined relative triality-sector energies [9, §§24–25]. Those results do not supply a bound for all vacuum-orthogonal states. A nonzero-triality gap or string-tension lower bound also leaves the zero-triality excitation spectrum to be controlled.

The later global gauge-measure paper supplies a positive-measure and reconstruction architecture, with explicit conditions on consistent histories, the Euclidean transfer, global topology and regulator removal [21, §§45–46B, IXA-8, 50.0]. It also retains the global sector-coercivity and uniform-gap requirements separately. A candidate positive wall term or a retained record-subalgebra positivity result cannot substitute for the complete physical transfer and excitation bound. Thus the newer measure results strengthen the route without closing the missing all-state spectral inequality.

The explicit continuum construction in Section 10 closes the corresponding limit passage for its smaller Gaussian family. It does not establish the missing physical colour Hamiltonian or transfer identification. Likewise, a source relaxation rate or local record-stability eigenvalue is not automatically a physical energy in the chosen time units.

12 Validation and reproducibility

The accompanying computational package contains ten independently executable suites. The identities and inequalities above provide the mathematical conclusions; numerical work checks their implementation, normalisation and stated examples. No measured mass chooses an input, no interacting four-dimensional SU(2) or SU(3) ensemble is generated, and no new Yang–Mills loop coefficient is claimed.

Suite	Executed verification
Coarse graining	4D derivative spectra and alias sums; real-space Schur complements; exact SU(2) character transfer and Haar quadrature; truncation and scale-transport controls
Information and live records	85 coherence/Holevo cases; recording-speed family; joint covariance checks; nonlinear integration; oscillator-memory basis convergence
Source-based spectrum	503 checks covering the residual Hessian, gauge null direction, all polarisation blocks, constrained nullspaces and transfer quadrature
Volume and continuum	396 checks including complete small-box real-space spectra, bounded inertia, unit conversion, resolvent convergence and smeared vacuum covariance
Action and blocking controls	23 checks for periodic total derivatives, covariance subtraction, the four-dimensional oscillation counterexample, quartic scaling, rare-region eigenvalues and the positive-perturbation counterexample
Complete loop constraint test	111 checks of cycle and gradient ranks, finite record preservation, real-space constrained spectra, sufficient extra constraints and soft-mode scaling
Common restoring and inertial response	997 checks of symbolic reductions, mixed metrics, spectral response, continuity, the internal precursor, finite-step reconstruction and the general soft-mode bound
Corpus refinement and physical carriers	98 checks: 47 of exact grouping, reversibility, retained responses and the vanishing fine relaxation gap; 51 of cut/cycle spaces, sharp addresses and native neutral/charged reference prescriptions
Pinning, inertia and hidden spectra	226 checks of pinning polynomials, all-momentum bounds, algebraic-current limits, coupled hidden transitions and exact spectral decomposition
Native current and fibre control	5,582 checks: general soft-lock determinant; full current elimination; transverse dispersions and gap bounds; 300 random reversible lumpable chains; temporal reflection positivity; physical-unit scaling

The 500 algebraic and quadrature comparisons in the source-spectrum suite have maximum absolute discrepancy 1.55×10^{-14}; its three finite-size asymptotic checks use a separate 10^{-6} tolerance. The continuum suite has maximum comparison discrepancy 1.15×10^{-10}. The action and blocking controls uses explicitly labelled tolerances, including an asymptotic fourth-order-scaling comparison; it does not present all errors as floating-point roundoff.

Full real-space matrices were diagonalised on small periodic boxes with sides two, three and four. Large sizes, up to side 131072 on the joint continuum path, use the proven dispersion minimiser rather than allocated three-dimensional matrices. The analytic bound covers intervening sizes and momenta. The covariance integral passed a 72-versus-96-node check; its Gaussian tail outside $|k_i| \leq 6$ is bounded below 10^{-17}.

The complete-loop suite has maximum residual 2.14×10^{-14}. The common-response suite has maximum residual 1.71×10^{-9} from a numerical frequency derivative, within its recorded tolerance. These are algebraic and implementation checks, not independent physical admission evidence.

The corpus-refinement checks have maximum retained-pair discrepancy 4.98×10^{-14}; the carrier identities have maximum residual 4.31×10^{-16}. Their native input arrays are included with their hash. The cycle refinement is a constructed control, and its gap is a Markov relaxation gap. None of these numerical checks establishes its physical admission or supplies a quantum Yang–Mills spectrum.

The pinning and hidden-spectrum suite verifies 226 comparisons, including generalized eigenvalues with variable current inertia, the singular algebraic-current limit, finite-pinning positivity and monotonicity, and an endpoint-dependent hidden transition. The analytic proofs cover intermediate parameters; the finite checks verify the formulas and their implementation. Source coverage and the section-level reading log are supplied separately in the supplement.

The native-current and fibre-control suite adds 5,582 checks with seed 20261111. Its 300 chains verify exact spectral splitting and the within-fibre lower bound on the original clock. The gap and branch formulas are compared against direct Schur complements and eigenvalues for 80 general coefficient sets. Finite reflection-positive Gram matrices check the temporal covariance identity. The largest discrepancy, 1.25×10^{-8}, is a finite-parameter small-pinning asymptotic comparison within its declared tolerance, not a roundoff claim. Analytic proofs, rather than these finite tests, establish the general theorems.

Run python supplement/run_all.py with NumPy, SciPy, SymPy and Matplotlib. The source, continuum and constraint suites use seed 20261109; common response uses 20261110. The corpus-refinement suite is deterministic. The package contains scripts, CSV data, validation, plots, sources and checksums. Python, python-docx and Pandoc build the paper with native Word equations.

13 The remaining physical derivation

The corpus already supplies a common action, native record effects, covariant current response and exact protection of the complete retained response under compatible refinement. It also identifies the HX1 phase within the master action and proves that minimal renewal cannot regenerate it. The remaining task is to apply these results on the actual physical carrier. The declared spatial phase parent has a soft collective direction, whereas the native neutral flat-transport family of Section 7.2 is gauge. Hard relative-phase locking or fixed positive pinning gives the conditional Abelian Gaussian continuum gap. The coefficient and kinetic scales must be returned by physical dynamics, not selected to reproduce that gap. Physical completion requires the following links.

Physical admission. Pull the complete committed-record constraints back to the joint current–matter–record variables at the selected preparation or vacuum. Include the dynamics of every comparison reference and the physical Gauss constraints. Determine whether the candidate directions are forbidden, gauge redundant or admitted. The selected sharp primitive carrier alone does not answer this continuous tangent-space question, and a gauge direction needs no additional energetic lock.

Common physical dynamics. Return the full operational kinetic operator, measure and joint interaction on the admitted space. Apply the common-kernel or spectral formulas of Section 9 to those returned data, retaining all mixed terms, temporal memory and fluctuations once. On a reversible Gaussian branch, a returned full joint transition and its covariance provide an executable alternative. The primitive kinetic coefficients must not be fitted to the target gap.

Uniform energetic control. Establish the resulting restoring-to-inertia bound in physical units along refinement. If N spans the physical constrained tangent space after gauge quotient, the quadratic target is

$$N^{\dagger}KN \succcurlyeq m_*^2 N^{\dagger}MN, \qquad m_* > 0 \text{ uniformly in volume and regulator.}$$

The bound must cover all physically admitted refinement directions. Lemma 4.3 splits retained and hidden relaxation spectra exactly; Proposition 4.5 supplies a checkable sufficient bound from a uniform within-fibre gap on the source clock. The maximal faithful quotient removes continuation-invisible distinctions. Apply the fibre test to the actual admitted source, then establish its relation to the physical transfer energy; a relaxation estimate alone is not a quantum mass. For the Gaussian pinning route, Section 11.1 now specifies the coefficient-selection and refinement questions for c, ρ and the field inertia.

Interacting vacuum and physical theory. Include the remaining non-Abelian, matter, record and measure contributions with fluctuations counted once. Prove the relevant vacuum and correlation or transfer bounds, and establish their continuum passage. If pure Yang–Mills is the target, demonstrate the correspondence to that theory rather than introducing additional physical fields that change it. Reflection positivity, the physical observable algebra and relativistic reconstruction must be addressed at that level [1].

The spectral version of the final goal is a uniform contraction on the physical vacuum complement, with a_t the physical time step and exact blocking by b steps:

$$\| T_{a_t,R}^{b}(I - P_{\mathrm{vac}}) \| \leq e^{-b a_t \Delta_*}, \qquad \Delta_* > 0.$$

Together with the appropriate nontrivial limiting construction and vacuum control, this gives the physical gap. Establishing one scalar correlator or one sector lower bound is insufficient to cover every physical channel. A numerical pilot should therefore use matched gauge-invariant correlation matrices, autocorrelation-aware errors, volume scans and physical scale setting; exact temporal blocking must leave the extracted energies invariant.

Conclusion

Commitment constraints can support a spectral gap under explicit dynamical assumptions. Finite pinning joins the soft Abelian Gaussian parent to the hard-locked Stueckelberg-type limit. Algebraic elimination of the current gives the exact two-field mass formula and relativistic transverse dispersions when the gradient coefficients match; the longitudinal sector remains nonrelativistic. Compatible reversible refinement splits retained and hidden relaxation spectra, and a uniform fibre Poincaré bound controls the hidden part. The Gaussian continuum families have a unique vacuum, positive gap, time reflection positivity and temporal clustering. Their mass scale remains an input. A physical derivation must return the coefficients and kinetic normalization on the admitted carrier, protect their physical scaling and control the interacting non-Abelian theory. The conditional results do not yet establish the pure Yang–Mills mass gap.

Appendix A Disposition of the superseded claims

The following dispositions apply to both earlier papers. Their useful definitions and conditional analytical tools are retained where used explicitly above. Their stronger conclusions are superseded by the results and hypotheses in this paper.

Earlier claim or inference	Consolidated disposition
The integral of the Laplacian of tr F^2 is a bulk mass-producing dimension-six interaction	Withdrawn; it is a total derivative under the stated boundary conditions
A nonnegative variance proves a positive entropy coupling	Withdrawn; the exact blocked Hessian contains a covariance subtraction and projections need separate matching
Positive good-site density and mixing imply the global gap	Withdrawn; rare empty regions provide counterexamples
Average absolute gradient controls maximum block oscillation in four dimensions	Replaced by a valid supremum-gradient or stronger Sobolev bound
Positive local derivative stiffness survives joining blocks as a bulk gap	Withdrawn; explicit nonconstant soft modes survive
Positive weights or finite-range blocking automatically provide all reconstruction properties	Not assumed; reflection structure and generated interactions require control
One unqualified existence hypothesis closes the entropy-modulated Yang–Mills proof	Withdrawn; physical identification, spectral control and limit construction have distinct requirements
Glueball masses of 1.9 ± 0.3 GeV or 1.5 ± 0.5 GeV follow from the mechanism	Withdrawn as predictions; the present results are in reference units
The commitment mechanism can yield a stable conditional gap	Retained in the precise Gaussian form of Theorems 8.1 and 10.1

Appendix B Auxiliary currents, kinetic geometry and measure

B.1 Auxiliary-current reconstruction

The required current reduction can be stated without an external working note. In matched real coordinates, let j denote all independent current components and z the remaining matter, link and record coordinates. The local constitutive and continuity defects of the master action [13] have the form $D_J = j - F(z)$ and $D_T = \dot{r} + B_U j$. They contain no separate j in this restriction. This makes j auxiliary in the local defect action; it does not determine whether the complete operational kinetic operator [15] adds current derivatives or mixed terms.

At frequency ω, write the positive supported joint precision as

$$\mathcal{Q}(\omega) = \begin{pmatrix} A_j & B_j(\omega) \\ B_j(\omega)^\dagger & D_z(\omega) \end{pmatrix}, \qquad \Gamma_z = D_z - B_j^\dagger A_j^{-1} B_j.$$

Gaussian completion and block inversion give the conditional current and full current covariance:

$$\mathbb{E}[j \mid z] = -A_j^{-1} B_j z, \qquad \mathrm{Cov}(j \mid z) = A_j^{-1},$$

$$\mathcal{G}_{jj}(\omega) = A_j^{-1} + A_j^{-1} B_j \Gamma_z^{-1} B_j^\dagger A_j^{-1}.$$

Proof. Complete the square with $j + A_j^{-1} B_j z$, then invert the remaining Γ_z block. If A_j is frequency independent its first term is a contact covariance in time; the second inherits the poles and memory of the coupled coordinates. If operational dynamics makes the blocks frequency dependent, the same identity holds with that dependence retained. A singular block needs its supported inverse and compatible range. A separately added current noise would change this covariance unless it has already been included in the common precision.

Continuity also explains why imposing $B_U j = 0$ can remove legitimate dynamics: the actual condition is $B_U j = -\dot{r}$. A compensated density change need not be a divergence-free current. On a connected graph with E edges, V vertices and representation dimension r_{rep}, rank-nullity gives

$$\dim\ker B_U = r_{\mathrm{rep}}(E - V) + \dim\ker D_U, \qquad B_U = D_U^\dagger.$$

The kernel of D_U consists of parallel vertex sections and is identified at a root with vectors fixed by every loop holonomy. Its dimension can change with the links. Hard projection onto the moving cycle kernel can therefore discard weakly longitudinal motions; keeping the full current and continuity coupling avoids that inference. Sections 9.5 and 9.6 supply explicit reductions, including the complete four-coordinate matrix and its response poles. They are self-contained declared Gaussian restrictions, not a selection of the missing physical kinetic operator.

B.2 The complete coordinate metric and reference measure

Let upstream operational amplitudes ζ carry metric g_{op} and density $r_{\mathrm{op}} d\mathrm{vol}_{g_{\mathrm{op}}}$. For a supplied configuration embedding $\zeta = F(q)$, the pullback metric is

$$G_{AB}(q) = \mathrm{Re}\langle \partial_A F, \partial_B F \rangle_{g_{\mathrm{op}}}.$$

This follows by substituting $d\zeta = DF\, dq$ into its norm. All mixed current–matter–record blocks come from the same Jacobian. The induced geometric volume is $\sqrt{\det G}\, dq$; an independently inherited density

also remains. A carrier embedding that makes operators well typed need not supply this complete configuration map.

For coarse observables $q = Q(\zeta)$ with derivative B_Q, the projected covariance of a diffusion with principal symbol g_{op}^{-1} is $A_q = B_Q g_{\mathrm{op}}^{-1} B_Q^T$. On its full-rank supported image, the minimum-norm horizontal lift and metric are

$$E_Q = g_{\mathrm{op}}^{-1} B_Q^T A_q^{-1}, \qquad G_q = E_Q^T g_{\mathrm{op}} E_Q = A_q^{-1}.$$

The lift solves $B_Q E_Q = I$ by minimizing the upstream norm. It defines an autonomous diffusion only if its symbol and drift descend along each unresolved fibre, or a justified reduction keeps the resulting memory. Coarea gives the pushed density in coordinate volume:

$$w(q) = \int_{Q^{-1}(q)} \frac{r_{\mathrm{op}}(\zeta)}{\sqrt{\det A_q(\zeta)}}\, d\mathrm{vol}_{g_{\mathrm{op}},\mathrm{fibre}}(\zeta).$$

If A_q is constant on a fibre, this is $\nu_{\mathrm{fibre}}(q)\sqrt{\det G_q(q)}$. A changing fibre volume contributes to the reversible drift. Given the metric and this reference density, integration by parts yields the symmetric scalar kinetic operator

$$H_{\mathrm{kin}} = -\frac{\hbar^2}{2w}\partial_A(wG^{AB}\partial_B).$$

Bundle connections and physical ordering terms must be supplied when present. The eventual ground-state probability density does not replace the reference measure in this operator.

For a coordinate change, set $\eta_J = J - F(\xi)$ and $L_F = D_\xi F$. Even a declared product metric $\mathrm{diag}(M_\xi, M_J)$ in (ξ, J) becomes

$$G_{\xi\eta_J} = \begin{pmatrix} M_\xi + L_F^T M_J L_F & L_F^T M_J \\ M_J L_F & M_J \end{pmatrix}, \qquad \det G_{\xi\eta_J} = \det M_\xi \det M_J.$$

The full triangular Jacobian has determinant one, which proves the determinant identity. Its mixed entries are required by coordinate covariance; omitting them changes the dynamics. Setting $\eta_J = 0$ is a restriction, not integration over the independent current departure. These formulas explain the metric and measure requirements used in Section 9 without assuming that the physical upstream metric is a product.

References

[1] A. Jaffe and E. Witten. Quantum Yang–Mills Theory. In The Millennium Prize Problems, Clay Mathematics Institute and American Mathematical Society, 2006. Official problem statement. Source

[2] K. Taylor. A Gauge-Invariant Entropic Mechanism for the Yang–Mills Mass Gap: A Rigorous Derivational Framework. Website edition, 83 pages. Superseded by the present paper. Source

[3] K. Taylor. Entropy–Convexity Constructive Clarification: Strengthening the Analytic Foundations of the Yang–Mills Mass Gap Program. Website edition, 108 pages. Superseded by the present paper. Source

[4] K. Taylor. Primitive Matter Selection in VERSF: Cumulative Executed Theorems on Fact Commitment, Record Retention, Renewal and R4-to-Charged-Flavour Descent. PMS-1-R126P-INTEGRATED. Especially PMS-EX58, §§28–29, and the carrier distinction in §30.7. Source

[5] K. Taylor. Physical Matter–Higgs Record Weighting and the Gauge-Coupling Closure Gate in VERSF. SGW-2. Especially §§13.2–13.5 and §17. Source

[6] K. Taylor. Source History Weighting and the Coarse-Grained Gauge Action in VERSF. Especially §18.11, Eq. (105); §19.5, Eq. (154); and §19.7, Eqs. (164)–(167). Source

[7] K. Taylor. The Post-Commitment Atomic Operation. Exact record invariance, §25; master-phase identification and minimal-renewal no-regeneration, §46R. Source

[8] K. Taylor. The Non-Perturbative QCD Scale and Triality Gap Completion Theorem in VERSF. Scope boundary §3.8, reference completion §§17–20, and physical projection target §20′. Source

[9] K. Taylor. GQSC-1R — The Faithful Quotient Retained Global Measure. Centre-transfer non-identifiability, §§24–25, Theorem 14 and Proposition 14.1. Source

[10] T. Baumgratz, M. Cramer and M. B. Plenio. Quantifying Coherence. Physical Review Letters 113, 140401 (2014). Source

[11] M. Zwolak, H. T. Quan and W. H. Zurek. Quantum Darwinism in a Mixed Environment. Physical Review Letters 103, 110402 (2009). Context for record information in environment correlations; no Yang–Mills claim is inferred from this work. Public preprint titled Quantum Darwinism in a hazy environment. Source

[12] K. Taylor. Physical Matter Record Dynamics and Gauge Response in VERSF. 62-page edition consulted 9 November 2026. §§15.7, 16.11–16.14 and 17.3–17.4. Source

[13] K. Taylor. The VERSF Master Substrate Action and Constitutive-Descent Theorem. Independent current, common constitutive and continuity defects, and the complete operational carrier. Source

[14] K. Taylor. Configuration Dynamics, Refinement Geometry and Record-Conditioned Curvature Response in VERSF. 130-page edition consulted 9 November 2026. IV.16–IV.17, particularly Eqs. IV.52–IV.58. Source

[15] K. Taylor. The VERSF History Measure Generation Geometry and Branch Closure Theorem. §4, §§8–10 and §56A. Operational geometry, the common heat sandwich and the physical input manifest. Source

[16] K. Taylor. The Renormalised Standard Model Parameter-Closure Theorem in VERSF. §71.2, correcting §67. The identity response of a minimum-norm defect lift is not physical coefficient selection. Source

[17] K. Taylor. From Fold to Three Generations in VERSF. §§19–21 on the neutral source and internal preparation; §§33–37 on exact retained-response preservation and its refinement scope. Source

[18] K. Taylor. The Fold-to-K7 Physical Stitching and Marked-Anchor Reduction in VERSF. §§10–17.5 on the actual trap attachment; §23B on sharp history addresses; §23N on co-terminal comparison. Source

[19] K. Taylor. The Twelve-Sector Current-Rigidity Source-Generated Rank-Six Theorem. RCHS-1, §§39A–39P. The six internal current modes and their native response derivatives. Source

[20] K. Taylor. Physical Applicability and Irreversible Response in VERSF. SGW-3, §42, Propositions 53–54: current-conservation reduction and neutral-source coupling. Source

[21] K. Taylor. The Substrate Cohomology Global Gauge Measure and Positive-Pushforward Strong-Phase No-Go Theorem in VERSF. §§45–46B, Theorem IXA-8 and §50.0. Source

[22] K. Taylor. The Ordered-Commitment χ Readout Theorem in VERSF. §§7.1–7.3: continuation-faithful coarse-graining and the maximal channel quotient. Source

[23] K. Taylor. The Primitive Field-Dependent Marked Instrument Programme in VERSF. §§65–71: the covariant source, native on-shell probability-rank certificate and declared persistent-ledger renewal. Source

[24] H. Ruegg and M. Ruiz-Altaba. The Stueckelberg Field. International Journal of Modern Physics A 19, 3265–3348 (2004). Abelian Stueckelberg and Proca formulations. Source

[25] T. Balaban, J. Imbrie, A. Jaffe and D. Brydges. The Mass Gap for Higgs Models on a Unit Lattice. Annals of Physics 158, 281–319 (1984). Theorem 4.1; weakly coupled Abelian Higgs model. Source

[26] K. Osterwalder and E. Seiler. Gauge Field Theories on a Lattice. Annals of Physics 110, 440–471 (1978). Rigorous lattice gauge and Higgs regimes. Source

[27] E. Fradkin and S. Shenker. Phase Diagrams of Lattice Gauge Theories with Higgs Fields. Physical Review D 19, 3682–3697 (1979). Fixed-length Higgs fields; public author preprint. Source

[28] E. Seiler. On the Higgs–Confinement Complementarity. arXiv:1506.00862 (2015). Author clarification of the weak-coupling Higgs regime and the uniform cluster-expansion argument. Source

The computational supplement contains the executable controls, source manifest and source-coverage notes. The current-reduction and kinetic-measure formulas needed here are derived in Section 9 and Appendix B; no private working-note link is required to follow those arguments.